UNIVERSITY OF CALIFORNIA, SAN DIEGO

Designing Novel Synthetic Enzyme-Like Structures with Inducible Dynamic Catalytic Properties

A thesis submitted in partial satisfaction of the requirements for the degree

Master of Science

In

Bioengineering

by

Michelle Lillian Cheung

Committee in charge:

Professor Michael Heller, Chair
Professor Shankar Subramaniam
Professor Xiaohua Huang

2012

The Thesis of Michelle Lillian Cheung is approved and it is acceptable in quality and form for publication on microfilm and electronically:

Chair

University of California, San Diego

2012

Dedicated to

My family and friends

We go where the science is, where the problems are, and karate the hell out of them."

-- Heller lab mission statement.

TABLE OF CONTENTS

LIST OF FIGURES

LIST OF TABLES

ACKNOWLEDGEMENT

This thesis would not have been possible without the guidance and the help of many individuals who in one way or another helped me in my completing my thesis.

First and foremost, I would like to thank Dr. Michael Heller for his patience and endless encouragements throughout my journey in exploring the field of synthetic enzyme mechanics. His weekly pizza, soda, and snacks had also been a constant source that propels me forward in research.

To my other committee members Dr. Shankar Subramaniam and Dr. Xiaohwa Huang for taking time out of the busy schedule to listen to my defense, to challenge my ideas, and to sign off one of the most important chapter of my life.

My sincere gratitude to Dr. Peter Chen, my mentor and friend since the beginning of my UCSD career. His patient, kindness, and wisdom have been invaluable to me. He never fails to support me and has enlightened me in many aspects of life. I am also very grateful to Dr. Anthony Cheung, Dr. David Gough, and Dr. Frank Talke for recommending me back to the UCSD Bioengineering program.

I am indebted to many of my colleagues for providing a stimulating and fun environment in which I can learn and grow. I am especially grateful to Tsukasa Takahashi, my project sidekick, who spent endless hours with me running experiments and has given so generously of his time to read/edit my manuscripts. Special thanks to the researchers I have had the privilege of working with: Avery “BOSS” Sonnenberg, Johnson Yu, Youngjun Song, Augusta Modestino, Mrudul Bhide, and Maria Hannson. Graduate school would not have been so pleasant without them.

To my family and friends who do not quite understand my research yet still have strong faith in my ability to graduate, thank you!

And most importantly, to my parents David and Judy, for raising me to be the person I am and for sending me aboard. Of equal importance, to Uncle Ben and Auntie Maddy, for taking in a kid who was at her most rebellious age and yet never cease giving her endless love and encouragement. To them I dedicate this thesis.

ABSTRACT OF THE THESIS

Designing Novel Synthetic Enzyme-Like Structures with Inducible Dynamic Catalytic Properties

by

Michelle Lillian Cheung

Master of Science in Bioengineering

University of California, San Diego, 2012

Professor Michael Heller, Chair

Over the past three decades considerable efforts have been made to create synthetic versions of enzymes, sometimes called *synzymes*. Most have failed, and the few so-called successes are at best only marginal exhibiting properties that can barely be described as catalytic. While these synthetic nano-structures look similar to the enzyme active site, they do not have the unique mechanical or dynamic catalytic properties to transform a substrate molecule into the desired product molecule with turnover

capability. In our study, a series of synzymes that mimics the active catalytic site of proteases which utilizes serine/hydroxyl, cysteine/sulfhydryl, histidine/imidazole and aspartate/carboxyl groups were designed and fabricated. The acetylation and the deacylation kinetics of the synzyme peptides were studied through molecular modeling and UV/Vis spectrophotometry. The intramolecular interactions of synzyme residues were measured with proton NMR. These synzymes were shown to be able to hydrolyze p-nitrophenyl acetate esters and acetic anhydride. Synzymes with phenylalanines between the cysteine and histidine yield a significantly higher deacylation rate, suggesting that the large bulky R-groups of phenylalanine bends the backbone of the synzyme, thus bringing the cysteine thiol group and the histidine imidazole group closer for acetyl exchange. When oscillating pulse electric field was applied to the synzymes, an increase in acetylation rate is observed, suggesting the possibility that PEF treatment aids the electroconformation change of the synzyme during the catalysis process, which in turn increased its deacylation ability and turnover rate.

CHAPTER 1: INTRODUCTION

Of all the magnificent macromolecules in living organisms, enzymes represent those which are the most complex in terms of mechanistic and sterochemical properties. Enzymes are able to catalyze the transformation of all other biomolecules, providing the dynamics and very essence of life (Hunter)(Bachovchin)(Fricker) . In these new days of nanotechnology, enzymes can aptly be considered natural bio-nanomachines that do chemistry. These bio-nanomachines catalyze reactions with high specificity and enormous rate accelerations that might otherwise be kinetically prohibited, with some having turnover rate of million substrate molecules per second (Kisailus et al.).

The catalytic triad is thought to be primarily responsible for efficient catalysis. For serine protease with the motif consisting of Ser/His/Asp, the serine acts as a nucleophile, histidine is the general base and acid, and the aspartate helps orient the histidine residue and neutralize the charge that develops on the histidine during the transition states (Ekici, Paetzel, and Dalbey). With the aid of a hydrogen bonding network within the reaction site, the triad functions as a cyclic charge relay mechanism where protons are thought to be exchanged from one residue to another, hence a very efficient turnover mechanism. Without such complex stereochemical fit between enzyme and substrate as well as the hydrogen bond network surrounding the triad, efficient enzyme catalysis will not be possible.

In recent years, there has been an ever growing need to use synthetic enzyme (commonly known as synzyme) in pharmaceutical industry, medicine, energy, and nano-fabrication (Liao et al.). Sadly, while the synzymes are based on peptide, macromolecule and nanostructures that are designed to closely resemble the active site of an enzyme, the few so-called successes are at best only marginal exhibiting properties that can barely be described as catalytic (Kisailus et al.). A number of artificial enzymes have been reported catalyzing various reactions with rate increases

up to 10^3 fold, which is still substantially lower than natural enzymes that typically cause rate increases above 10^6 fold.

Heller et. al. observed the existence of a rapid, reversible intramolecular transfer of the acetyl group between cysteine and histidine residual which the acetyl group is more attracted to the cysteine residue, preventing the synzyme from turning over. Hence, mechanism inhibiting the back-attack of the cysteine group would allow for an efficient deacylation to occur through an intramolecular nucleophilic catalysis by the imidazole group (Heller, Walder, and Klotz). Leveraging off these findings, we explored synthetic enzyme designs and their kinetics under various conditions in search for a stable, reusable synzyme using a combination of serine, cysteine, histidine and aspartic acid. We also explored the effect of oscillating electric field to the synzyme that would temporary induce a conformation change for a more efficient, controllable acetyl-exchange during catalysis. If successful, modified enzyme that mimics the original enzyme catalytic ability might be able to deliver a degree of optimization that was not previously attainable, creating a paradigm shift for various field of research.

CHAPTER 2: BACKGROUND

2-1. Proteases

Proteases, also known as proteinase or peptidases, are proteolytic enzyme that cleaves long amino acid into shorter fragments. They can accelerate hydrolytic reactions up to 10^{10} times (Kraut). They are heavily involved in a multitude of physiological reactions ranging from cell-cycle progression to immune response by controlling protein size, composition, shape, and degradation. Therefore, proteases are often targeted by pharmaceutical industry for disease treatments (Deu, Verdoes, and Bogyo).

There are six types of proteases that are categorized by their catalytic mechanism. They are: aspartic, cysteine, glutamic, metallo, serine, and threonine (Rawlings, Morton, and Barrett). For our study, we focus on the catalytic reactions of serine and cysteine protease. Though they are structurally distinct from each other, they carry out analogous reactions. The key residues for the serine protease are aspartic acid, histidine, and serine. The hydroxyl group of serine functions as a nucleophile and the imidazole ring of histidine functions as a general acid/general base during catalysis. Similarly, the active site of the cysteine proteinases also involves three key residues: asparagine, histidine, and cysteine. The thiolated anion of the cysteine functions as a nucleophile during the initial stages of catalysis (Beveridge). In contrast, other proteases activate water molecules to initiate catalysis reactions.

A. Catalytic triad

The protease catalytic reaction is a highly specific mechanism. Each protease requires specific environment condition for splitting specific amino acid sequences (Shen and Chou). The main site that is responsible for the enzyme's proteolytic activity is known as the catalytic triad. Its ubiquitous occurrences emphasize the importance of structural motif and side group

interactions. The catalytic triad of the cysteine protease papain consists of Cys-25, His-159, and Asp-175 while serine protease chymotrypsin contains Ser-195, His-57, and Asn-102. The location of the triad varies with the individual protease but together, they are hidden in a network of deep hydrophobic pocket that is highly specific to the shape of the substrate region to be cleaved.

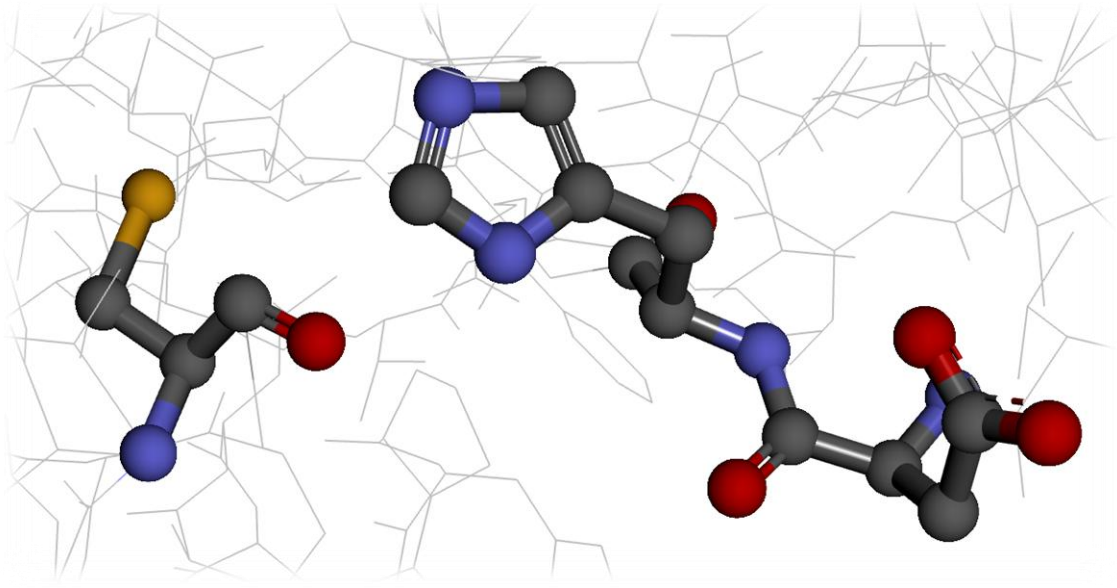

Figure 1 - The catalytic triad of papain (cysteine protease), which comprise of Cys-25, His-159, and Asp-158.

B. Catalytic mechanism of Serine and Cysteine proteases

The catalytic reaction of proteases can be separated into two half reactions: 1) acetylation where the peptide substrate is cleaved by the protease and the formation of an intermediate structure and 2) deacetylation where the protease hydrolyzes the cleaved substrate and restore to its original state (Nelson, David, Cox).

i. Acetylation

When the substrate binds to the enzyme, it is positioned within the hydrophobic pocket of the enzyme that is made for the bond cleaving reaction to occur. In serine proteases, the

interaction of serine and histidine generates a strongly nucleophilic alkoxide ion on serine, the ion attacks the peptide carbonyl group, forming a tetrahedral acyl-enzyme (ES complex). This is accompanied by the formation of the short-lived negative charge on the carbonyl oxygen of the substrate, which is stabilized by the oxyanion hole. The collapse of the intermediate due to the unstable negative charge leads to a new formation of a new intermediate and the breaking of the peptide bond. An incoming water molecule is deprotonated by general base catalysis, generating a strong nucleophilic hydroxide ion. Attack of the hydroxide on the ester linkage of the acyl-enzyme generates a second tetrahedral intermediate, with oxygen in the oxyanion hole again taking on a negative charge (Janowski).

Similarly, cysteine proteinases operate through the formation of an acyl-enzyme intermediate which is a thiol ester, whose formation and decomposition are assisted by a histidine residue. This charge distribution resembles the ion-pair formed during catalysis by the parent serine enzyme, i.e. charge distribution of the negatively charged tetrahedral adduct and the protonated histidine (Polgár and Halász).

ii. Deacetylation

The collapse of the tetrahedral intermediate then displaces the serine. The subtle change in the conformation compresses the hydrogen bond between histidine and aspartic acid, resulting in a stronger interaction called a lower-barrier hydrogen bond. This enhance interaction by increasing the pKa of the free histidine from 7 to >12, allowing the histidine residue to act as an enhanced general base that can remove the proton from the serine hydroxyl group.

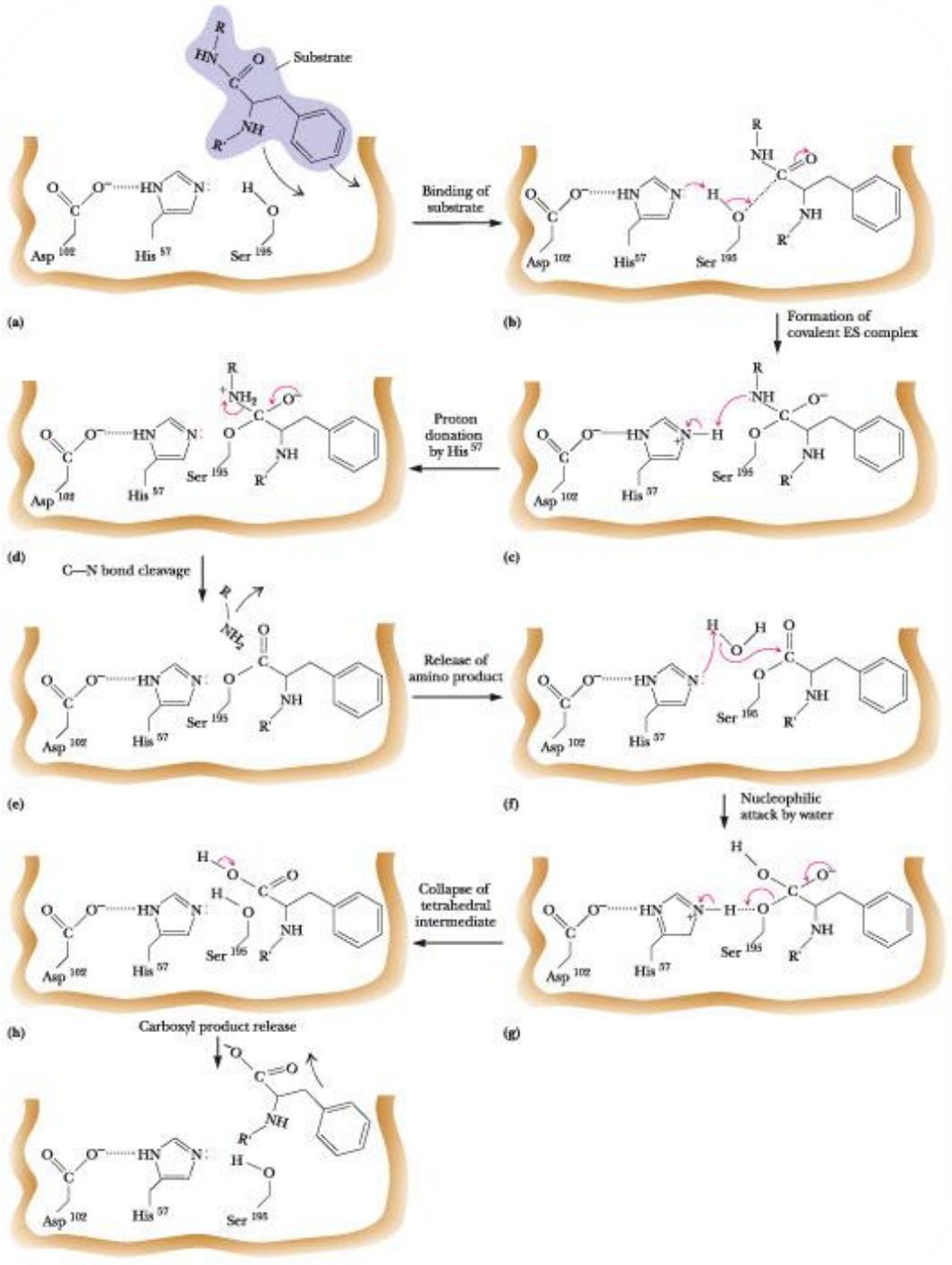

Figure 2 - The mechanism of Chymotrypsin (serine protease) catalysis.

C. Charge relay mechanism

Protease charge relay mechanism during acetylation and deacylation plays a significant role in dictating protease catalysis ability as it controls the triad charge redistribution that is needed for an efficient acetyl deacylation. At neutral pH, serine's hydroxyl group is not very reactive. However, in this charge relay mechanism, it is proposed that the negative charge of the aspartic acid is transferred to serine through a series of hydrogen bond, forming a very reactive alkoxide anion for the initiation the cleaving mechanism.

In the process of relaying charges, the enzyme will oscillate between different conformation states while proton being transferred from one residue to another, varying the intramolecular distance between each triad functional group as well as their free energy states that favor the catalysis reaction. Although there has been a debate on whether the catalytic mechanism was a full or partial proton transfer (Polgár and Halász), it is agreed upon that charge relay mechanism does enhance the nucleophilicity the nuclophilicity of the substrate attack. The proton is then transferred to the imidazole of histidine through a series of hydrogen bond, while the transfer of proton from histidine to aspartic acid can be considered as the first step of the alkoxide anion of serine as such transition is energetically favorable. Figure 3 - **The charge relay mechanism with its structural charge, intramolecular distance, and energy of serine protease.**below details the charge relay mechanism with its structural charge, intramolecular distance, and energy (Banacky, P, Linder) .

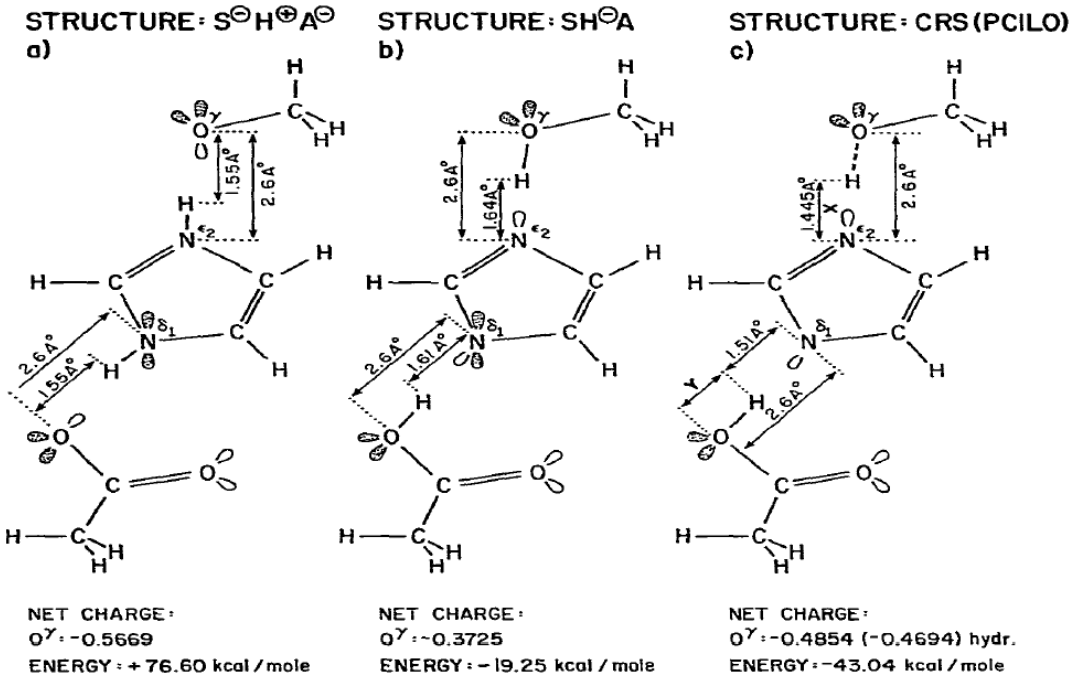

Figure 3 - The charge relay mechanism with its structural charge, intramolecular distance, and energy of serine protease.

D. Previous work with synthetic proteases

Recently, Dan Morse et. al. studied the catalytic mechanism and the essential participation of specific serine and histidine residues in silicatein's catalytic active site and sought to develop a synthetic mimic that provides both catalysis and template ability. Morse bounded the histidine and serine residue on solid chip that approximate the proximity of silicatein as shown in Figure 4 - Schematic of the essential chemical moieties in a silicatein, a serine-hydrolase active site. and Figure 5 - Schematic of the self-assembled monolayer done by Morse et. al.. Nevertheless, marginal hydrolytic ability is observed due to the lack of turnover ability (Kisailus et al.).

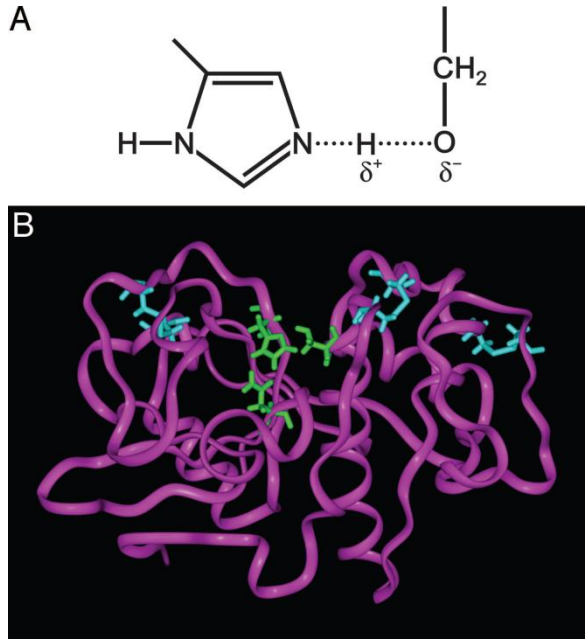

Figure 4 - Schematic of the essential chemical moieties in a silicatein, a serine-hydrolase active site.

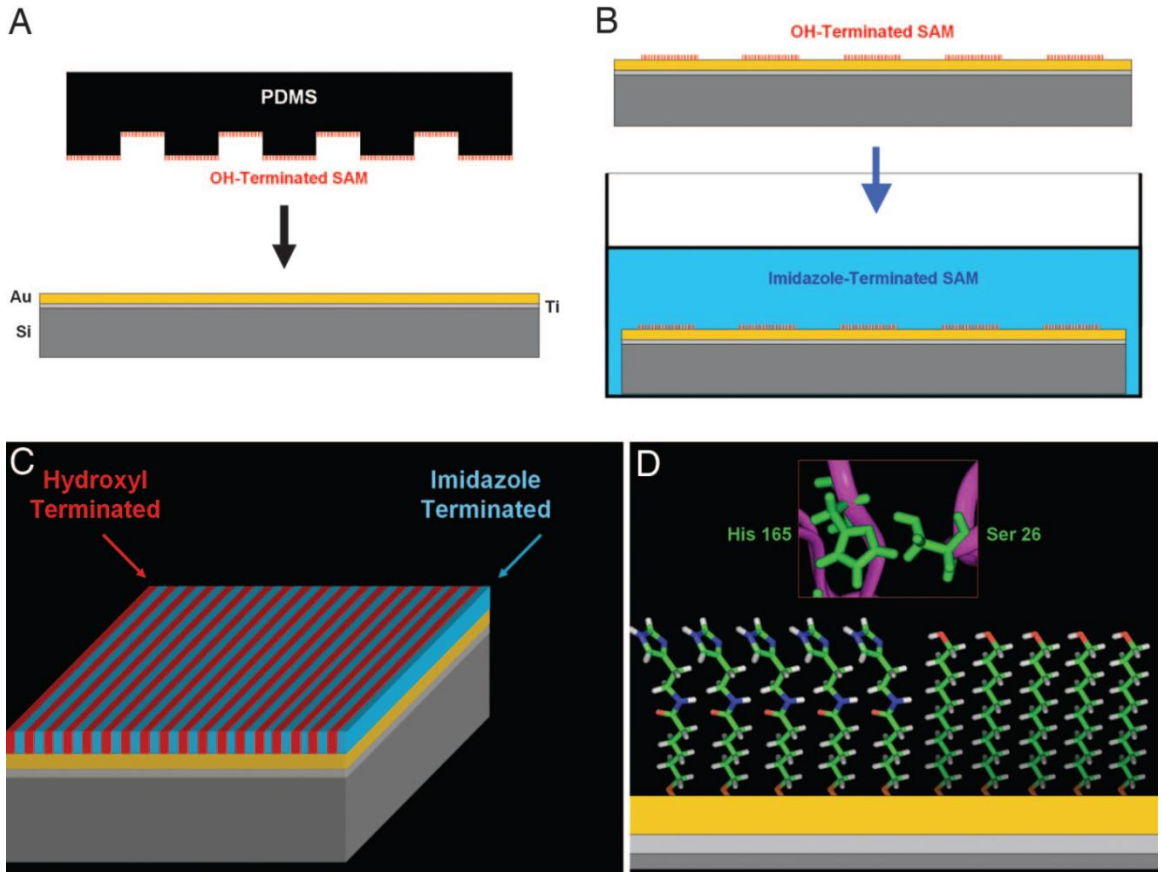

Figure 5 - Schematic of the self-assembled monolayer done by Morse et. al.

In a previous study done by Michael Heller et. al., his study in synthetic enzyme observed a rapid, reversible intramolecular transfer of the acetyl group between the cysteine and histidine which greatly favors cysteine. The acetyl back-attack mechanism described in Figure 6 – Acetyl back-attack mechanism between the acyl-thiol and acyl-imidazole intermediate in synthetic enzyme. demonstrated proximity alone cannot yield any catalytic ability in synthetic enzyme system (Heller, Walder, and Klotz).

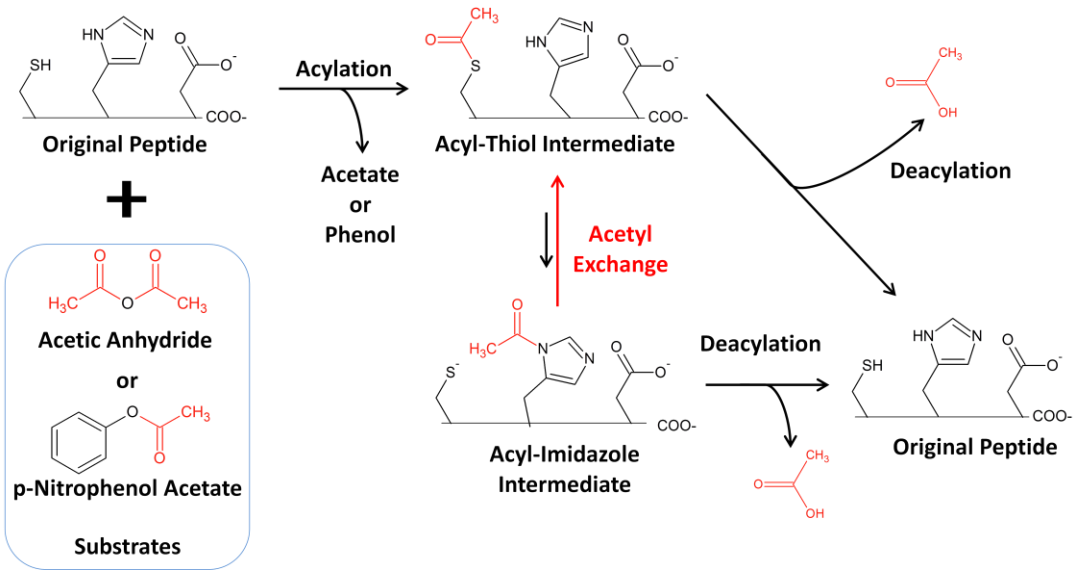

Figure 6 – Acetyl back-attack mechanism between the acyl-thiol and acyl-imidazole intermediate in synthetic enzyme.

Hence, Heller et. al. proposed using electric field to separate the cysteine (thiol) and histidine (imidazole) containing catalytic peptide sequences that were immobilized onto the surface of a solid surface (Heller, Michael (Nanogen), Tu, Eugene (Nanogen), Sosnowski, Ronald (Nanogen), O'Connell, James (Nanogen)). They proposed that the use of electric perturbation at its resonance frequency of acetyl-exchange would allow for an efficient deacylation mechanism (Figure 7 - **Diagram of peptide structure containing an arrangement of nucleophilic group designed to carry out electronic perturbation catalysis, hydrolysis, and deacylation.**).

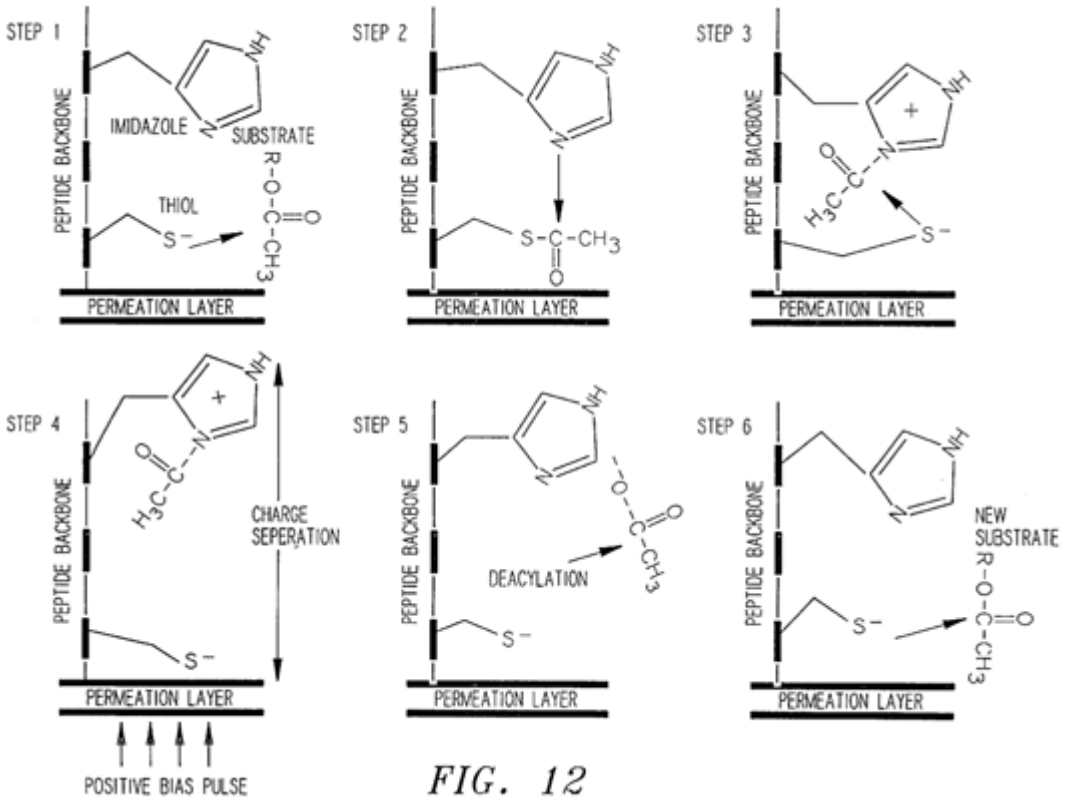

FIG. 12

Figure 7 - Diagram of peptide structure containing an arrangement of nucleophilic group designed to carry out electronic perturbation catalysis, hydrolysis, and deacylation.

Homogenous Enzyme Kinetics

In many reactions, the rate of reaction changes as the reaction progresses. The reaction rate is high initially and slowly plateaus as time increases. To characterize the reaction kinetics, we can describe them with differential rate law. The differential rate law relates the rate of reaction to the concentrations of the various species in the system.

A. Zero-Order Reaction

For a zero-order reaction, the rate of reaction is a constant. When the limiting reactant is completely consumed, the reaction stops abruptly. The reaction goes as below:

$$A \rightarrow Product$$

Differential Rate Law: $r = k$

The rate constant, *k*, has units of mole L^{-1} sec^{-1}.

B. First-Order Reaction

For a first-order reaction, the rate of reaction is directly proportional to the concentration of one of the reactants. The reaction goes as below:

$$A \rightarrow Product$$

Differential Rate Law: $r = k$ [A]

The rate constant, *k*, has units of sec^{-1}.

C. Second-Order Reaction

For a second-order reaction, the rate of reaction is directly proportional to the square of the concentration of one of the reactants or the product of two reactants. The reaction goes as below:

$$2A \rightarrow Product$$

or

$$A + B \rightarrow Product$$

Differential Rate Law: $r = k$ $[A]^2 = k$ [A] [B]

The rate constant, *k*, has units of L $mole^{-1}$ sec^{-1}.

The three rate order reactions are illustrated below.

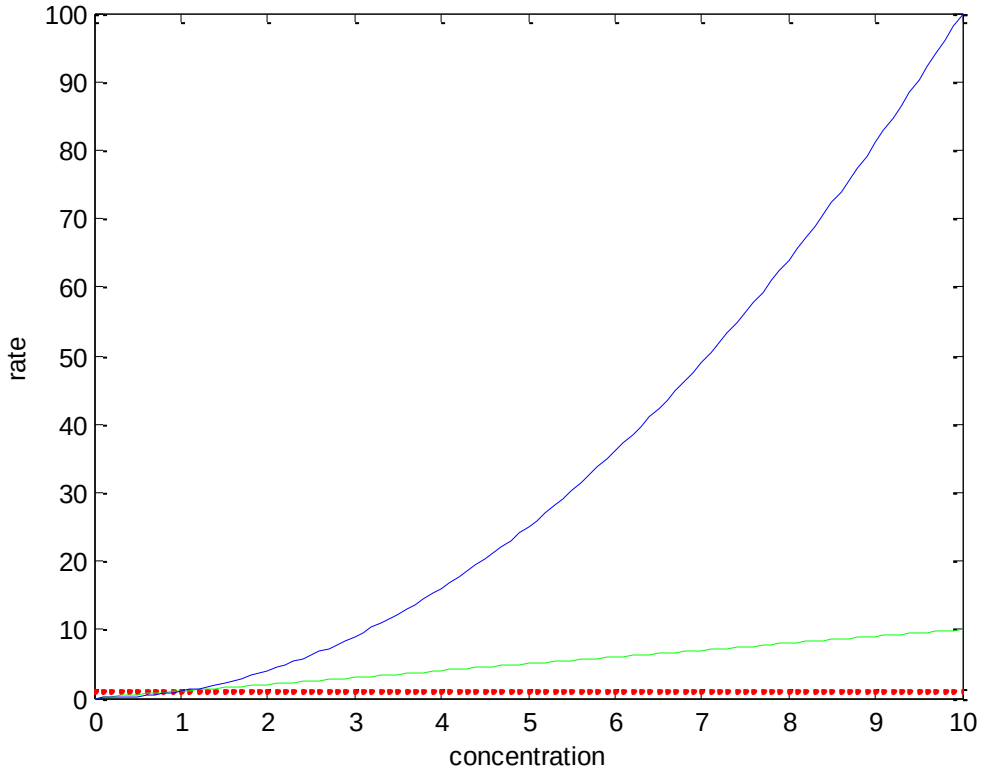

Figure 8 - Reaction rate VS reactant concentration of zero, first and second order reactions.

D. Michaelis-Menten Mechanism

Enzymatic cyclic behavior can be described by a simplified Michaelis-Menten model. It involves an enzyme E binding to a substrate S to form a complex ES, which in turn is converted into a product P and the enzyme. This may be represented schematically as:

$$E + S \overset{k_f}{\leftrightarrow} ES \overset{kcat}{\longrightarrow} E + P$$

Where E is the enzyme, S is the substrate, and ES is an enzyme-substrate complex.

And the rate can be described as:

$$v = \frac{d[P]}{dt} = \frac{V_{max}[S]}{K_m + [S]}$$

V_{max} represents the maximum rate achieved by the system at maximum (saturating) substrate concentrations. The Michaelis constant K_m is the substrate concentration at which the reaction rate is half of V_{max} and the equilibrium constant of the reaction is:

$$K = \frac{k_1}{k_{-1}}$$

2-2. Electrophoretic and Electrokinetic Theory

Three major electric field effects and phenomena that occur when an electrode is place in an aqueous solution and a voltage is applied:

A. DC < 1 volt

→ Nernst Layer Effects and Electrochemistry

At low DC field, charged molecules that are not being oxidized or reduced will organize themselves in a manner where a small ion concentration gradient is from on the surface of the electrodes and the bulk concentration region is constant after that region.(Kopeliovich)

B. DC = 1 volt

→ alignment of molecule

At 1V DC, field strength is sufficient to exert enough torque to align the molecule.

C. DC > 1 volt

→ H_2O Electrolysis and Electrophoretic Effects

At 1V DC or higher, molecules move in an electric field of field strength E depending on their net charge, molecular mass and shape. The smaller the mass or the larger the charge,

molecules move more rapidly toward the electrode of the opposite charge. At the electrodes, decomposition of water into hydrogen and oxygen will also begin.

The migration of the charged compound in a homogenous electric field can be described by:

$$F = z * e_0 * E$$

Where:

z = charge number of the compound

e0 = elemental charge [1.602*10^-19 As = C]

E = electric field strength (V/cm)

D. AC > 100 Hz

→ Dielectrophoretic Effects

In a non-uniform electric field, a dielectric force will be exerted on a dielectric particle. Depending on the particles' electrical properties and the medium it is suspended in, field strength, frequency, and size can manipulate particle the particle with great selectivity. This has allowed for the separation of cells or the orientation and manipulation of nanoparticles.

The total of the forces on a given particle is described by:

$$F_{total} = F_{deterministic} + F_{random}$$

Where:

$F_{deterministic}$ = the sum of the sedimentation, hydrodynamic and dielectrophoretic forces.

F_{random} = force due to Brownian motion (significant for nanoparticles).

The mean free path of the movement is inversely dependent on mass, implying that decrease in the particle diameter require significant increase in the applied electrostatic energy.

2-3. Electroconformation Coupling

Under strong electric field influence, molecules will behave differently from their zero field condition. Ion pairs will dissociate, dipoles will orient, molecules will be electronically and automatically polarized, and equilibria between different conformers of a protein will shifted (Tsong and Astumian). Previous studies had shown that proteases can act as a free energy transducer to harvest the energy from the oscillating field for its internal use (Tsong, Yow Tsong, Liu, Dao-Sheng, Chauvin). For a cyclic enzymatic process, an oscillating electric field can drive the reaction forward by providing an additional free energy source, decreasing the affinity of substrate to product or simply by slightly changing the conformation of substrate-enzyme complex. In the Michaelis-Menten model shown below, in order for the oscillating electric field to drive the reaction clockwise, T2 must possess an electric moment than its previous state T1 (Tsong, Yow Tsong, Liu, Dao-Sheng, Chauvin). It is important to note that the frequency of the applied field must match the kinetics of the enzyme. The optimal frequency of the field will be dependent on the rate of conformational change of during the conformational transition step. The field strength is also crucial as over exerting will lock the enzyme in certain state (Tsong, Yow Tsong, Liu, Dao-Sheng, Chauvin).

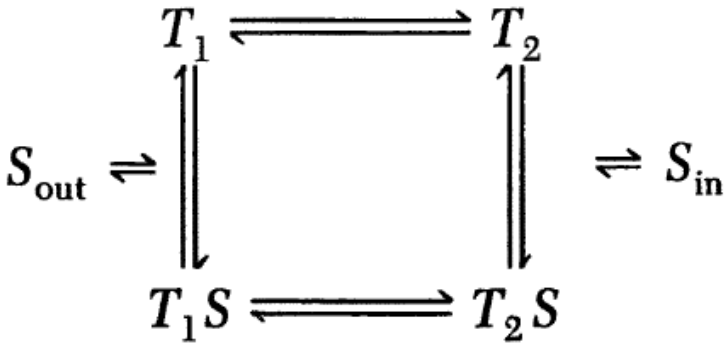

Figure 9 – A simplified four-state kinetic model for enzyme-catalyzed reaction.

Without considering buffer conductivity and viscosity as well as synzyme's dielectric property, the intramolecular electrostatic interaction of the charged acetyl-thiol and acetyl-histidine intermediate group during acetyl-exchange can be briefly approximate Coulomb's Law described by Figure 10 - Electrostatic attraction force of the charged acetyl-imidazole and acetyl-thiol group during the acetyl back-attack mechanism..

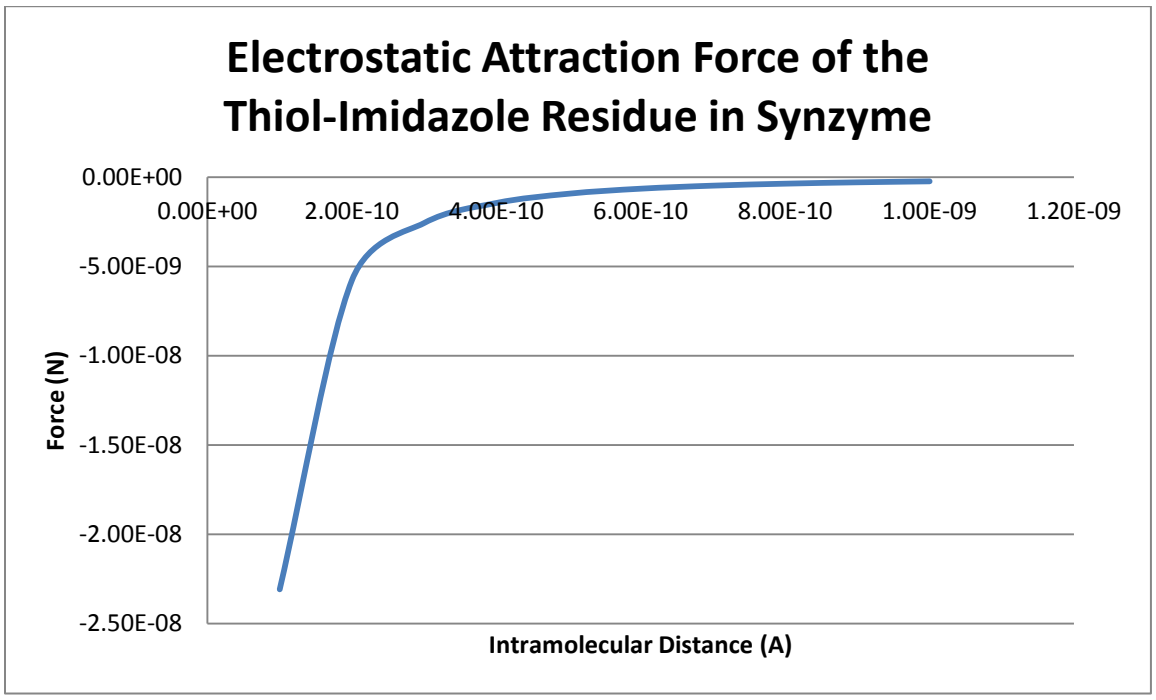

Figure 10 - Electrostatic attraction force of the charged acetyl-imidazole and acetyl-thiol group during the acetyl back-attack mechanism.

CHAPTER 3 – INSTRUMENTATIONS

3-1. Concentration Detection Via Ultraviolet–Visible Spectroscopy

Ultraviolet/visible (UV) spectroscopy is used extensively to measure the interaction of molecules with electromagnetic radiation. Using the energy at near-UV and visible range can promote electrons from ground state to an excited state. The spectrum measured from the absorption of light at the near-UV (150-400nm) and visible (400-800nm) provide useful information regarding the chemical nature, the molecular environment, and concentration of its chromophores. (Chemistry)

A. Spectrophotometers

The spectrophotometer uses two light sources: a deuterium lamp that emits light in the UV region and a tungsten-halogen lamp for the visible region. The light emitted from both lights are focused into the cuvette and the amount of light passes through the sample is detected by the photomultiplier or a photodiode. The absorbance of the sample is the difference between the light passes through the sample cuvette and the reference cuvette. The spectrophotometer can detect concentration as low as .0001mol/dm^3. The diagram highlights the main component of the instrument. The cuvette cells in the spectrometer are made of quartz for ultraviolet spectra.

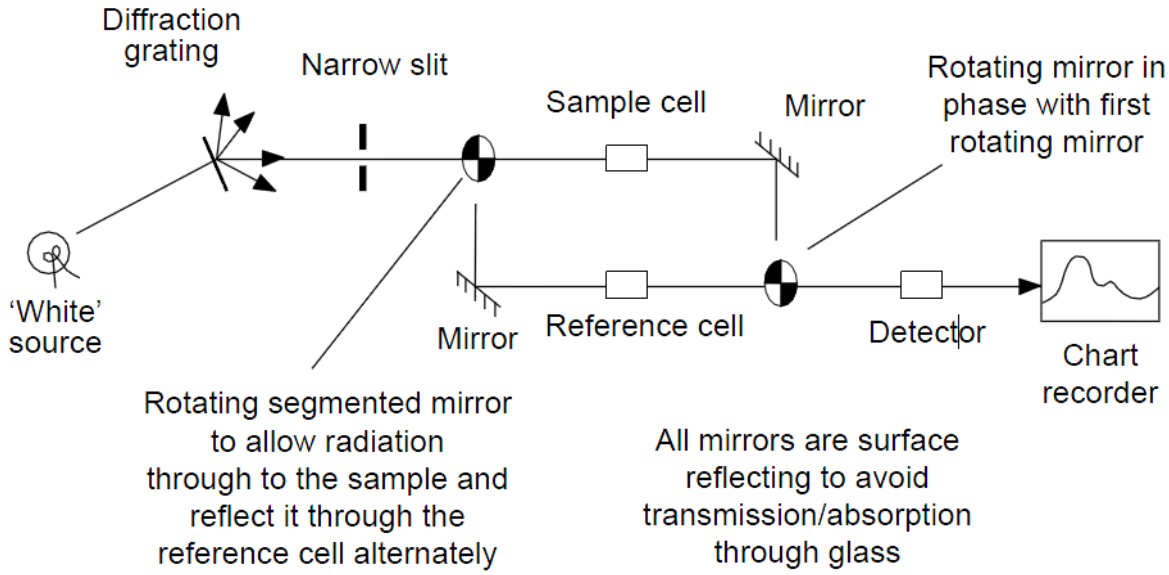

Figure 11 - Diagram of how UV-Vis spectrometer works.

B. *Absorption Calculation*

The concentration of the sample can be accurately determined by the absorbance measurements. The absorbance (A) is proportional to the ratio of the light intensity before and after passing the sample cell. At low absorbance, the Beer-Lambert Law relates the absorption of light through material which it is travelling as followed:

$$A = -\log_{10}(\frac{I}{I_0}) \text{ And } A = abc$$

Where:

A = absorbance

I = initial light

I0 = transmitted light

a = absorption coefficient of substance (L mol^{-1} cm^{-1})

b = path length of cuvette (cm)

c = molar concentration of species of interest (mol L^{-1})

3-2. Nuclear magnetic resonance spectroscopy

Nuclear magnetic resonance (NMR) spectroscopy is used to study molecular physics and structure. When molecule is placed in a magnetic field, NMR active nuclei such as ^{1}H and ^{13}C absorb the electromagnetic radiation at a specific frequency. (Techniques)("Nuclear Magnetic Resonance Spectroscopy")

The diagram below gives a schematic of a general 1-dimention proton NMR instrument:

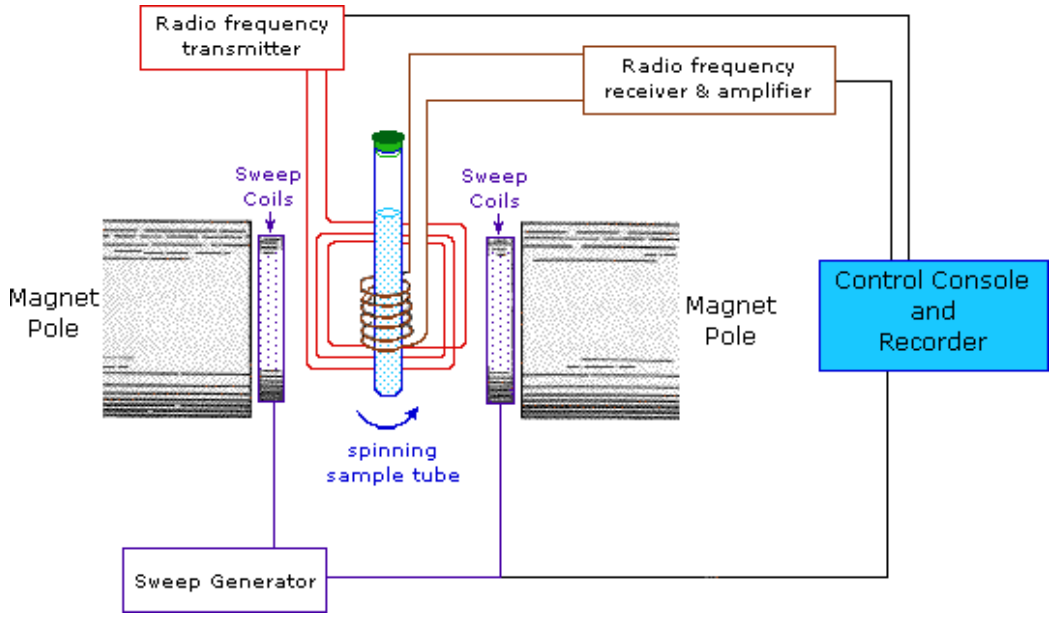

Figure 12 - Diagram of how NMR works.

The energy of a NMR transition depends on the magnetic-field strength and a proportionality factor for each nucleus called the magnetogyric ratio. The local environment around a given nucleus in a molecule will slightly perturbs the local magnetic field exerted on that nucleus and

affects its exact transition energy. This transition energy of NMR active nuclei in a molecule makes NMR spectroscopy extremely useful for determining the following:

i. The number of different types of hydrogen present in the molecule

Hydrogen attached to different atoms have different magnetic field. When electrons are withdrawn from a nucleus, the deshielded nucleus requires a stronger effective magnetic field (of higher frequency) to resonate. Generally, hydrogen bound to carbons attached to electron withdrawing groups tends to resonate at higher frequencies. Chemical shifting refers to the shift in position of where a particular hydrogen atom resonates relative to tetramethylsilane. The chart below illustrates the typical hydrogen resonance position relative to the atom it is attached to as well as the bonding. (NMRCentral)

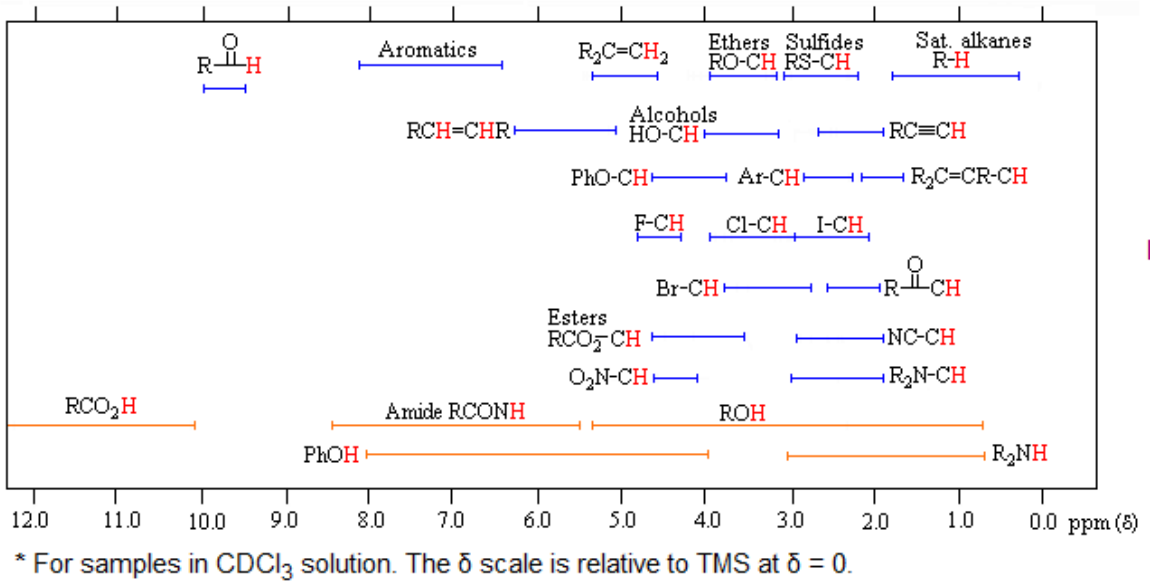

Figure 13 - 1D proton NMR Chemical Shift Range.

ii. The relative numbers of the different types of hydrogen

The area under the NMR resonance is proportional to the number of hydrogens which that resonance represents. By integrating the different NMR resonance, one can deduce the relative amount of chemically distinct hydrogen.

iii. The intramolecular electronic environment of the different types of hydrogen

Nuclear relaxation is determined by fluctuating magnetic field. When there are molecules in the proximity of the nuclei of interest that decrease its degree of freedom, which increase the relaxation time and increase the half-height linewidth of the peak. The inverse relationship of magnetic moment and intramolecular distance can be described by the Solomon-Blumberg equation (Holman):

$$T_{1M}^{-1} = T_{2M}^{-1} = \frac{4}{3}\left(\frac{\mu_0}{4\pi}\right)^2 \frac{\gamma_N^2 g_e^2 \mu_B^2 S(S+1)}{r^6} T_{1e}$$

Where:

S = magnetic moment

T1M-1 = T2m-1 = proton nuclear rates

T1e = tc. which is predominately the electron relaxation rate.

T1 = half-life

T1-1 = relaxation rate

iv. Information regarding the neighbor hydrogen

NMR resonance will split into N+1 peaks where N is the number of hydrogen on the adjacent atom. The intensity ratio of the resonance follows the Pascal's triangle ratio.

Table 1 - 1D Proton NMR splitting pattern

Number of Neighbor Hydrogen	Intensity Ratio	Number of Peaks
0	1	1 (singlet)
1	1:1	2 (doublet)
2	1:2:1	3 (triplet)
3	1:3:3:1	4 (quartet)

CHAPTER 4: EXPERIMENTAL PROCEDURE

4-1. MATERIAL

A. Synthetic Enzyme

11 synzymes containing a combination of Serine, Cysteine, Histidine, Aspartic Acid, and Aspartate were designed and synthesized by GeneScript. The key features that we vary in the designs are: 1) the spacer between the triad residues, for their side group can create a steric hindrance effect and change the intramolecular distance between the triad residues; 2) the residue on the N-terminal, for its R-group charge can increase the charge density on the N-tail, which strengthen alignment and movement of the synzyme in electric field, and 3) the order of the triad group, for the oscillation electric field should complement its electroconformation during catalysis.

All synzyme purities were above 90% and all designs are N-acetylated.

Table 2 - Sequence of Synzymes

	Sequence	Charge at pH 8.5
Synzyme 1	Gly-Gly-Ala-Ala-Cys-Ala-Ser-Ala-Asp	-2.5
Synzyme 2	Gly-Gly-Ala-Ala-Cys-Ala-His-Ala-Asp	-2.5
Synzyme 3	Arg-Gly-Ala-Ala-Cys-Ala-Ser-Ala-Asp	-1.5
Synzyme 4	Arg-Gly-Ala-Ala-Cys-Ala-His-Ala-Asp	-2
Synzyme 5	Arg-Gly-Ala-Phe-Cys-Phe-His-Ala-Asp	-1.5
Synzyme 6	Lys-Gly-Ala-Phe-Cys-Phe-His-Ala-Asp	-2
Synzyme 7	Arg-Asp-Phe-His-Phe-Cys-Ala-Gly-Asp	-2.5
Synzyme 8	Arg-Asp-Phe-Asn-Phe-Cys-Ala-Gly-Asp	-2.5
Synzyme 9	Arg-Asp-Phe-His-Phe-Met-Ala-Gly-Asp	-2
Synzyme 10	Arg-Asp-Phe-His-Phe-Ser-Ala-Gly-Asp	-2
Synzyme 11	Arg-Asp-Phe-Asn-Phe-Ser-Ala-Gly-Asp	-2

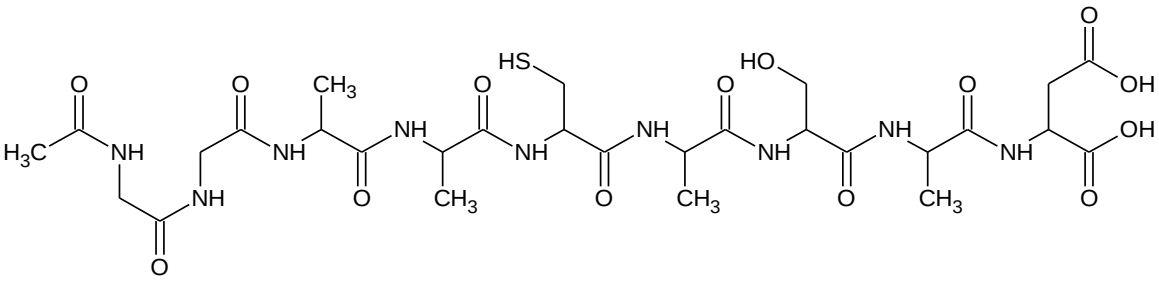

Figure 14 - Structure of synzyme 1.

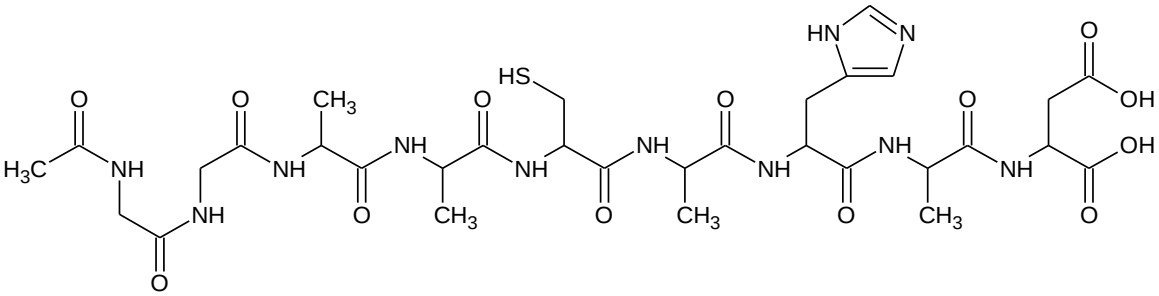

Figure 15 - Structure of synzyme 2.

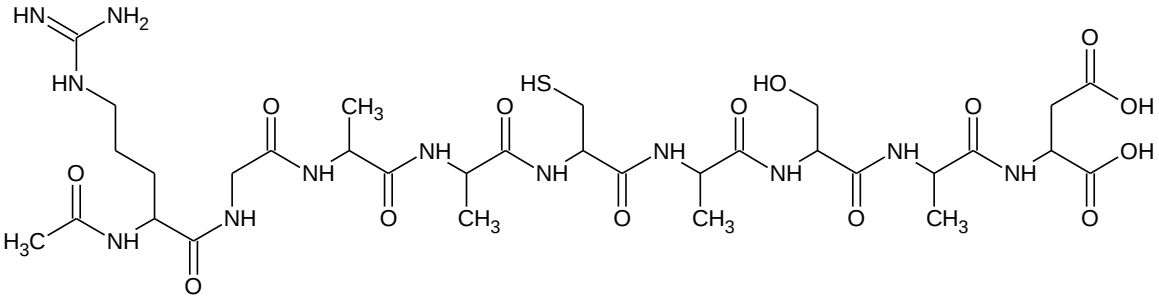

Figure 16 - Structure of synzyme 3.

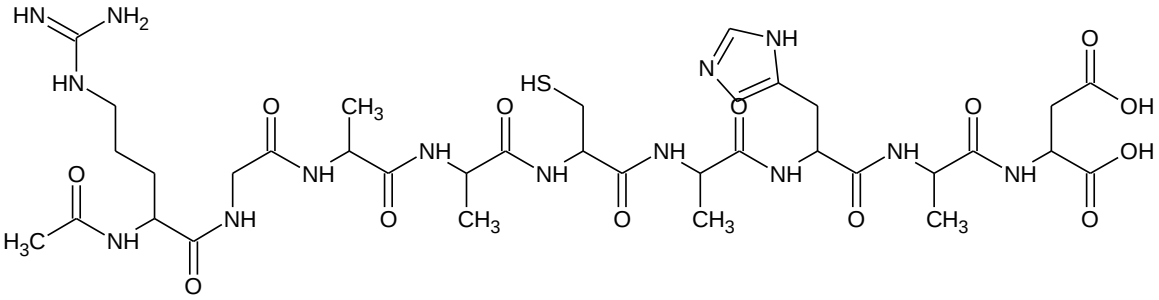

Figure 17 - Structure of synzyme 4.

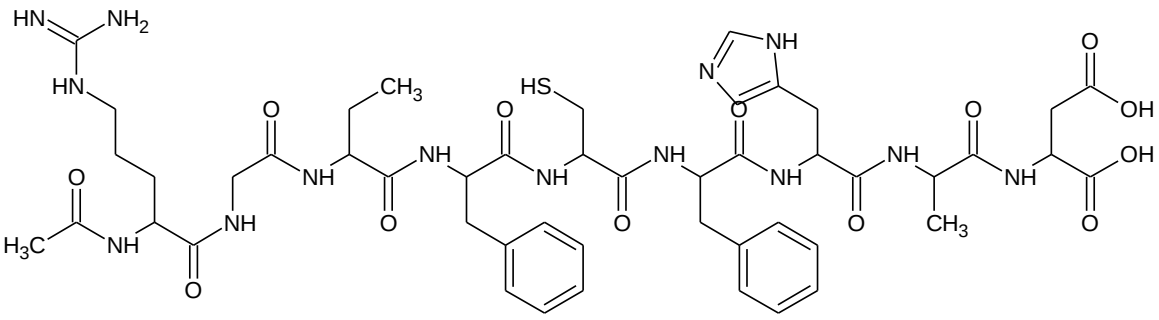

Figure 18 - Structure of synzyme 5.

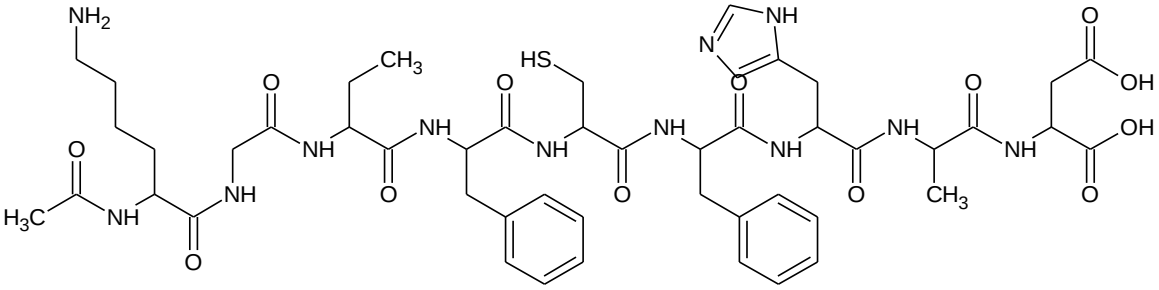

Figure 19 - Structure of synzyme 6.

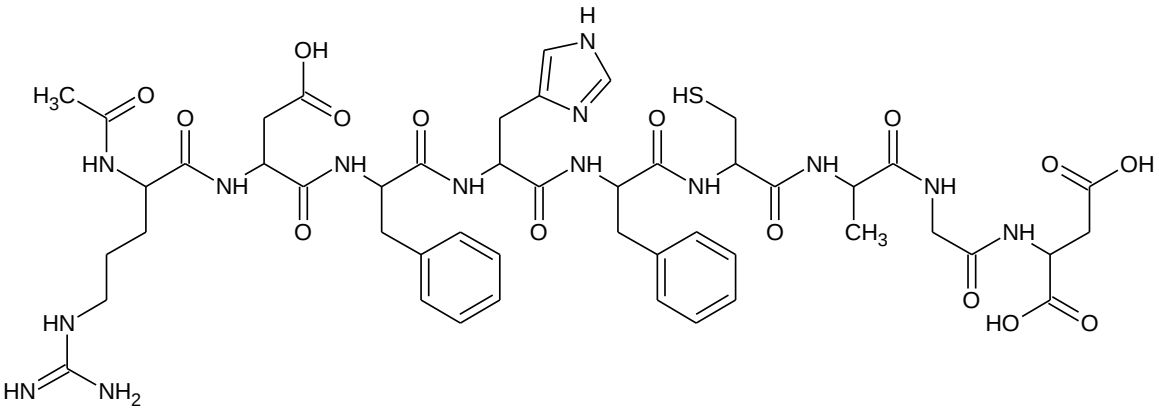

Figure 20 - Structure of synzyme 7.

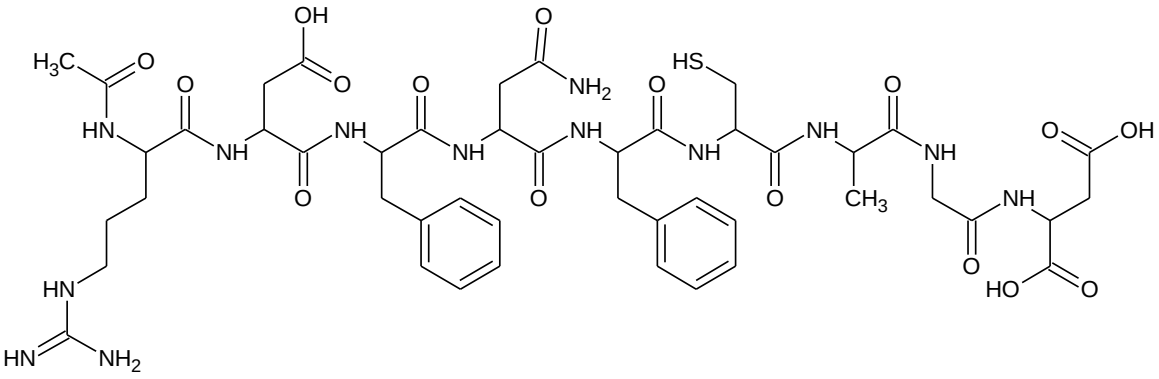

Figure 21 - Structure of synzyme 8.

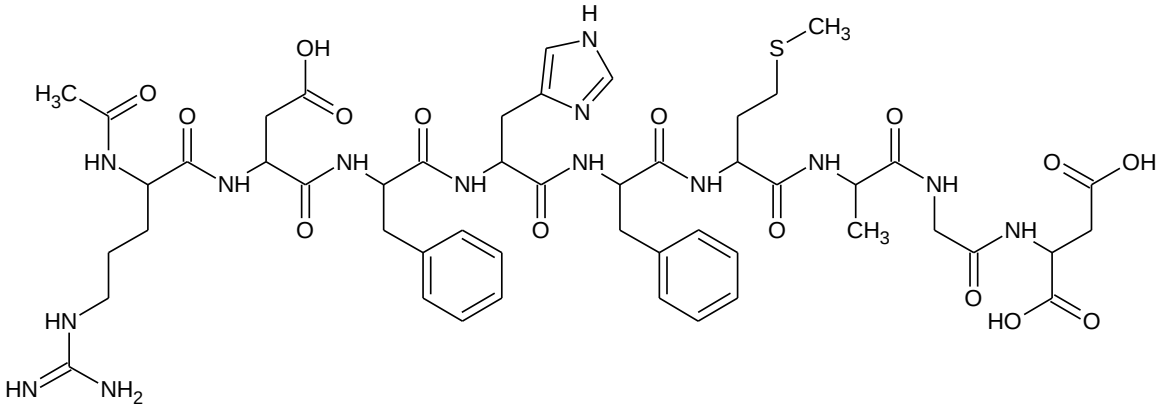

Figure 22 - Structure of synzyme 9.

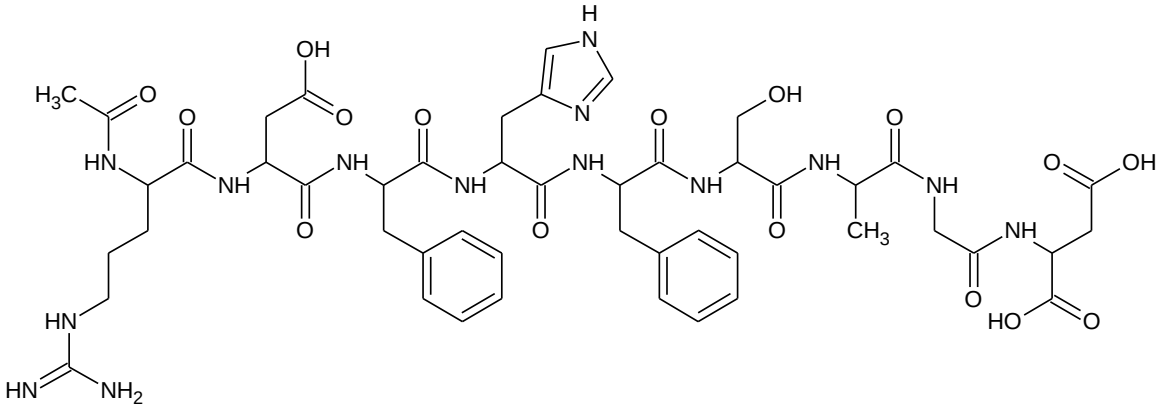

Figure 23 - Structure of synzyme 10.

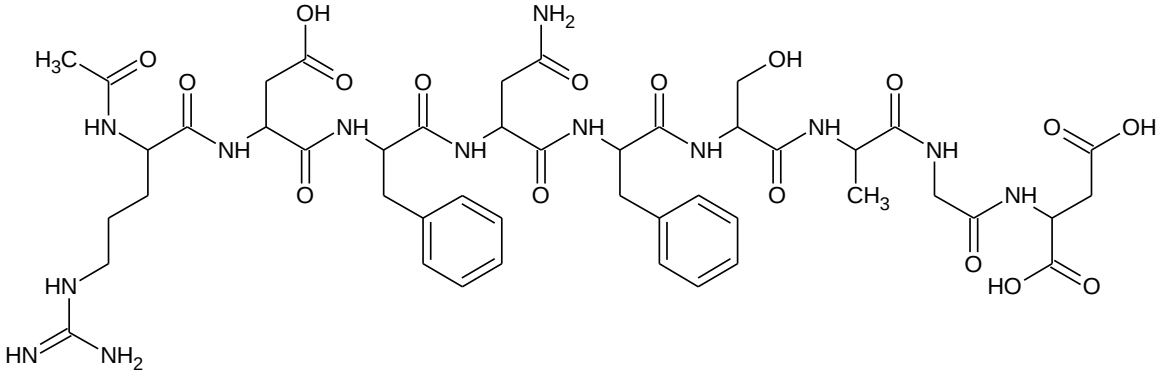

Figure 24 - Structure of synzyme 11.

B. Other Material and Solvents

Acetic anhydride was purchased from EMD Chemical USA and Acetonitrile was from Fisher Scientific. N-Acetyl-L Cysteine was purchased from Spectrum Chemical MFG Corp. N-Acetyl-L Histidine and p-nitrophenyl acetate were products of MP Biomedicals. Ellman's reagent (5,5'-dithiobis-(2-nitrobenzoic acid)) was obtained from G-Bioscience.

4-2. INSTRUMENTS

A. UV Spectrophotometer System

The system used for the research is Perkin Elmer Lambda 800 UV/Vis Spectrophotometer. Its light source came from pre-aligned tungsten-halogen and deuterium lamp with an UV/Vis resolution of 0.05nm. The UV WinLab software is used to processing the absorbance data from the spectrophotometer.

Basic Method of Operation:

All of the experiments run using the UV Spectrophotometer follow the same basic procedure. The steps are as following:

1. Insert 600ul of reference material into both sample and reference cuvettes for baseline detection.
2. Add in the reactant into the sample cuvette.
3. Measure the absorbance at a specific range of wavelength for a set period of time.

B. NMR

The system used for the research is the JEOL ECA 500 System. It uses a superconducting magnet that can produce field strength up to 500MHz. The system can detect 1-H or 19-F. Macintosh iMac is used for instrument control and data processing.

Basic Method of Operation:

1. Insert 500ul of sample into 5mm NMR tube.
2. Placed the NMR tube into the NMR System.
3. Measure NMR resonance after adjusting for coupling and other necessary parameters.

4-3. METHODS

A. Acetylation

The catalysis hydrolysis rates were studied by reacting the substrate p-nitrophenol acetate with N-acetyl L-cysteine, N-acetyl L-histidine, their combination, and with each of the synzyme 1-8. Acylation rate constants were determined by measuring the increase in p-nitrophenol absorbance at 400nm.

The synzyme-substrate reactions were examined at the pH of 8.5 in 0.1X Tris Borate buffer. The hydrolysis reaction of synzymes with p-nitrophenol acetate will yield p-nitrophenol, a chromic-effector with a yellow color change in the product. The absorbance intensity of the p-nitrophenol is proportional to the hydrolytic ability of the synzyme. The initiate rate and spontaneous rate were measured in a time span of 20 minutes. The reference spontaneous rate was the hydrolysis of p-nitrophenol acetate. The concentration of the substrate and the potential catalyst was 1E-4M. All experiments were performed at 25°C. Their cleavage reactions were followed with a Perkin Elmer Lambda 800 UV/Vis Spectrophotometer measuring the release of the corresponding cleaved p-nitrophenyl at 400nm. Second-order rate constant for the acylation process were determined from the initial rates according to the equation:

$$k_a = \frac{initial\ rate - spontaneous\ rate}{[catalyst][substrate]}$$

B. Deacylation

The deacylation studies were studied by reacting the substrate acetic anhydride with N-acetyl L-cysteine, N-acetyl L-cysteine, their combination, and with each of the synzyme 1-8. The synzymes were at a concentration of 1E-4M in 0.1XTB buffer at pH of 9.5 and were being acetylated with a 1.5E-3M of acetic anhydride (15-fold excess) injected as 10% solution in acetonitrile. The use of acetic anhydride for acetylation was to prevent later UV absorbance interference during the deacylation study. During the acetylation study, the acetyl-imidazole and the acetyl-thiol intermediate of the synzymes could be observed separately at 270nm and 235nm wavelength respectively. When acetylation reached equilibrium after 20 minutes as indicated by the non-changing absorbance of both acetyl intermediate complexes, the deacylation of the acetyl-thiol intermediate could be studied by adding Ellman's reagent 5 times the concentration of the synzyme. The addition of Ellman's reagent traps any free thiol from the deacylated acetyl-thiol intermediate, forming a disulfide bond that could not be back-attacked by the acetyl group from the acetyl-histidine intermediate. The cleaved product of Ellman's Reagent (2-nitro-5-thiobenzoate) gave out a yellow color that was measured at 412nm using UV spectroscopy. The increase absorbance of the cleaved Ellman's reagent was used to quantify the amount of deacylated acetyl-thiol complex. The reaction diagram is described as below in Figure 25. First-order rate constant for the deacylation process was determined with the initial rate initial rates according to the equation:

$$k_a = \frac{initial\ rate}{[catalyst]}$$

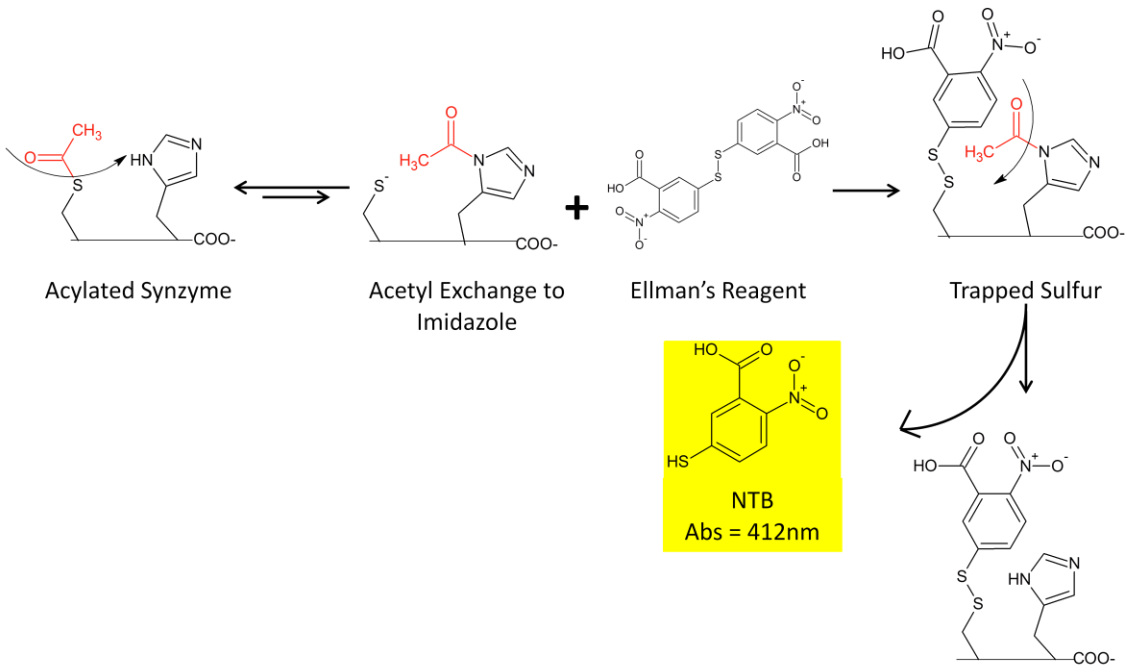

Figure 25 - Deacylation reaction with Ellman's Reagent.

C. NMR

1D Proton NMR spectra were obtained with JEOL ECA 500 NMR spectrophotometer. All spectra were recorded with 10% D20 and 90% deionized water as solvent with a water suppression treatment. The concentration of all synzymes and control recorded in the spectrum was approximately 1E-4M. All samples were prepared minutes before the experiment to minimize denaturation and oxidation. All spectra were taken using a spectral width of 500MHz. In order to observe higher proton resolution, spectra were recorded with a data size in time domain of 512 points. Water peak is suppressed from 4.5-5ppm for better signal to noise ratio.

D. Electric Field ** Proprietary Information for Thesis Review Only ***

The effect of electric field on synzyme catalytic ability was observed using p-nitrophenol acetate as a substrate. The enzyme-substrate was done in the same fashion as the acetylation study described in part A above with the addition of an external z-dimension oscillating electric field

induced to temporary conformational change to the enzyme. Glass Pasteur pipettes were filled with 5% agarose gels (dissolved in DI-water) and 1X PBS buffer was added on top of the gel to increase conductivity. Electric field was generated by Agilent 33210A Function Generator and Trek 2210 power supply and through platinum wires contacting the PBS buffer. The types of oscillating electric field tested include sine wave, square wave, pulsing, and arbitrary wave at various frequency and amplitude.

The simplified version of the experiment set-up is as below.

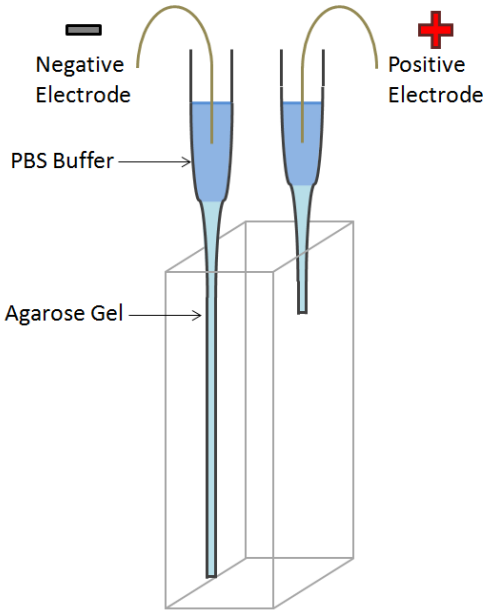

Proprietary Information
For Thesis Review Only

Figure 26 - Schematic of the gel electrodes for applying osilillating electric field. * Proprietary Information For Thesis Review Only ***

The mechanism of pulsing synzyme is shown in Figure 27 below. During the acetyl exchange between the thiol and imidazole group, there is a charge redistribution where the thiol is negatively charged while the imidazole is positively charged. We tried to take advantage of this phenomenon and apply electric field to separate the two functional groups. The electric field will pull the oppositely charged groups toward different directions and increase the intramolecular distance between them. We hypothesized that the increase in intramolecular distance aided the

acetyl group on the acetyl-imidazole intermediate to simply deacylate without back-attacking the thiol group, and hence a more efficient catalysis. By experimenting with various wave forms, frequency, amplitude, we hope to capture the resonance frequency when the acetyl-exchange occurs, and pull them apart at the right time with the proper amount force.

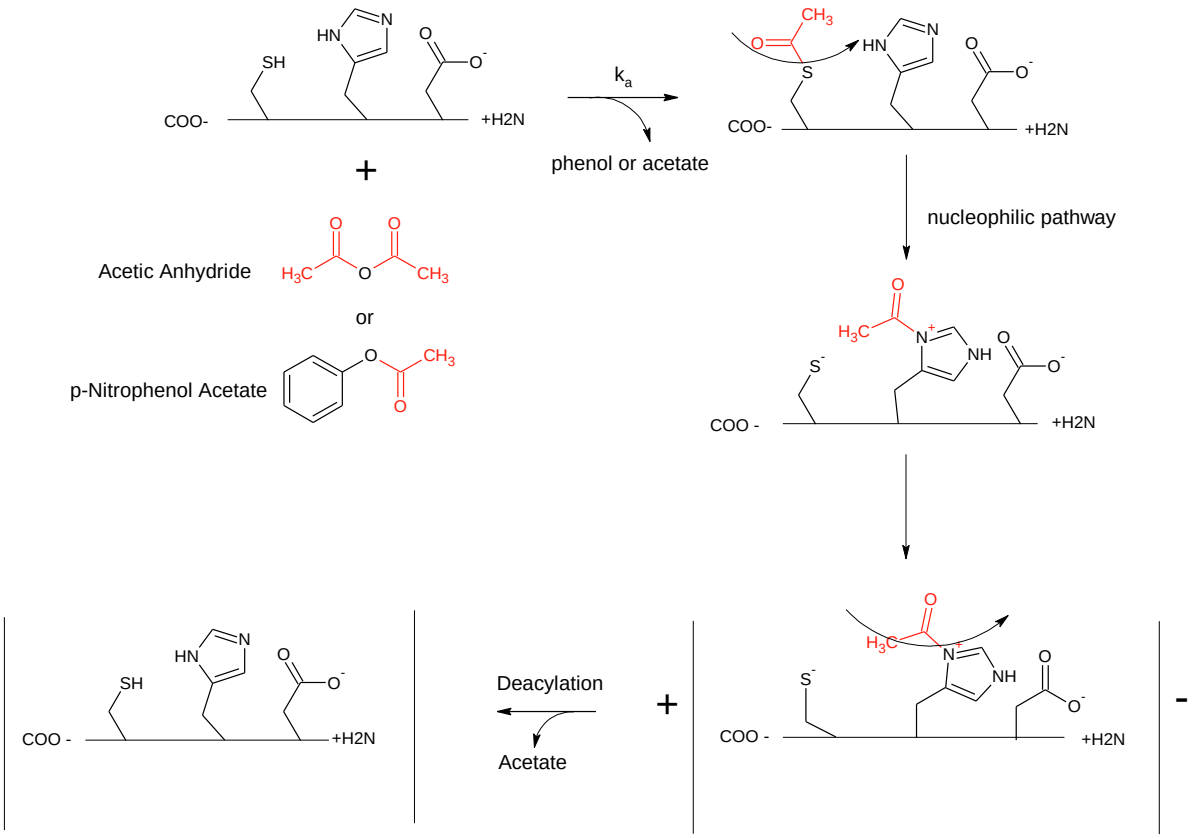

Figure 27 - Mechanism of pulsing synzymes.

CHAPTER 5: RESULTS

5-1. Acetylation

None of the synzymes acetylated with p-nitrophenol acetate at a rate significantly greater than the controls within the first 20 minutes of acetylation. The second order rate constant of each of the synzyme were calculated and shown in Figure 28.Figure 28 - Acetylation rate constant of various synzyme The controls on the right included the hydrolysis of p-nitrophenol acetate and its reaction with acetyl-cysteine, acetyl-histidine, and their combination. Minimal elevations in synzyme acetylation rate constants compare to the positive control of acetyl-cysteine reacting with p-nitrophenol acetate, suggesting synzymes had some marginal turnover capability.

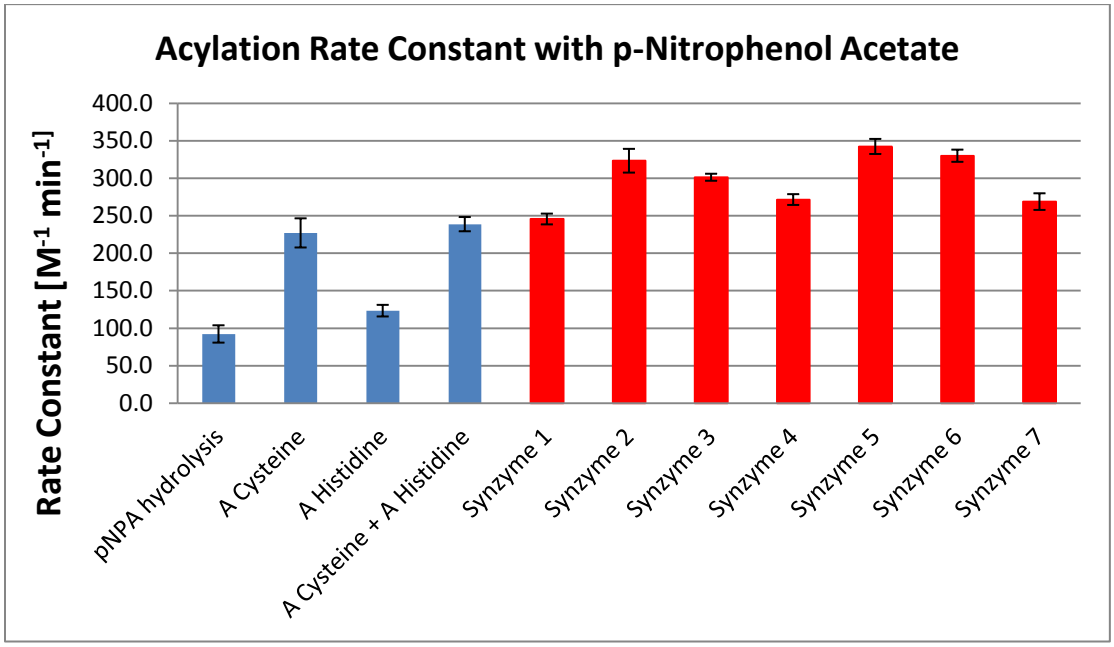

Figure 28 - Acetylation rate constant of various synzymes (in red) and controls (in blue) with p-Nitrophenol Acetate.

An alternative approach we took in studying acetylation is through acetic anhydride. Figure 29 shows the UV spectral change associated with the acetylation of synzyme 6 at time

points (in minutes) after the injection of acetic anhydride into sample cell. The absorption maxima at 270nm and 235nm correspond to the absorbance of acetyl-imidazole (histidine) and acetyl-thiol (cysteine) respectively. Within 30 seconds after the addition of substrate, the absorbance of both intermediate had already reached maxima and by 7.5 minutes, their acetyl exchange reached equilibrium. The baseline level of acetyl-imidazole intermediate in equilibrium reconfirmed the instability of the structure that the acetyl group tended to leave the imidazole either by deacylation or back-attack of the thiol.

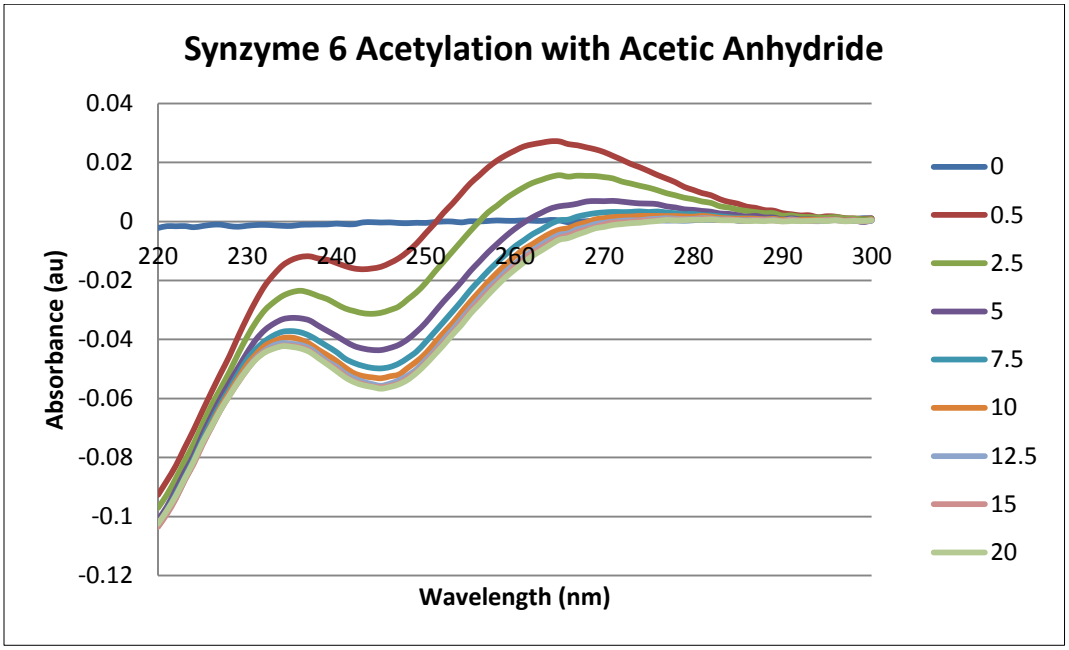

Figure 29 - UV spectral change associated with the acetylation of synzyme 6 at various time points (in minutes) after the injection of acetic anhydride into sample cell.

5-2. Deacylation

The deacylation rate constants were obtained by measuring the absorbance increase of the cleaved Ellman's Reagent. Figure 30 presented first order deacylation rate constant of synzymes in the Ellman's reagent trapping study. Synzymes with arginine at the N-terminal exhibited significant enhancement in deacylation rate compared to synzymes with glycine or lysine at the

N-terminal. Synzyme 5 and 6, with one phenylalanine in between the triad, deacylated at a much higher rate compared to the controls and synzymes with zero or two phenylalanine between the triad. This suggests minimal structural change in synzyme significantly influences catalysis rate. Synzyme 1 and 3, with cysteine and serine as part of the triad, appeared to be inert. The trapping effect of the Ellman's Reagent was only observed with cysteine-histidine synzymes reflected even in an extremely well-approximated intramolecular system, appropriate functional groups are essential in bring out the catalytic ability of the synzymes.

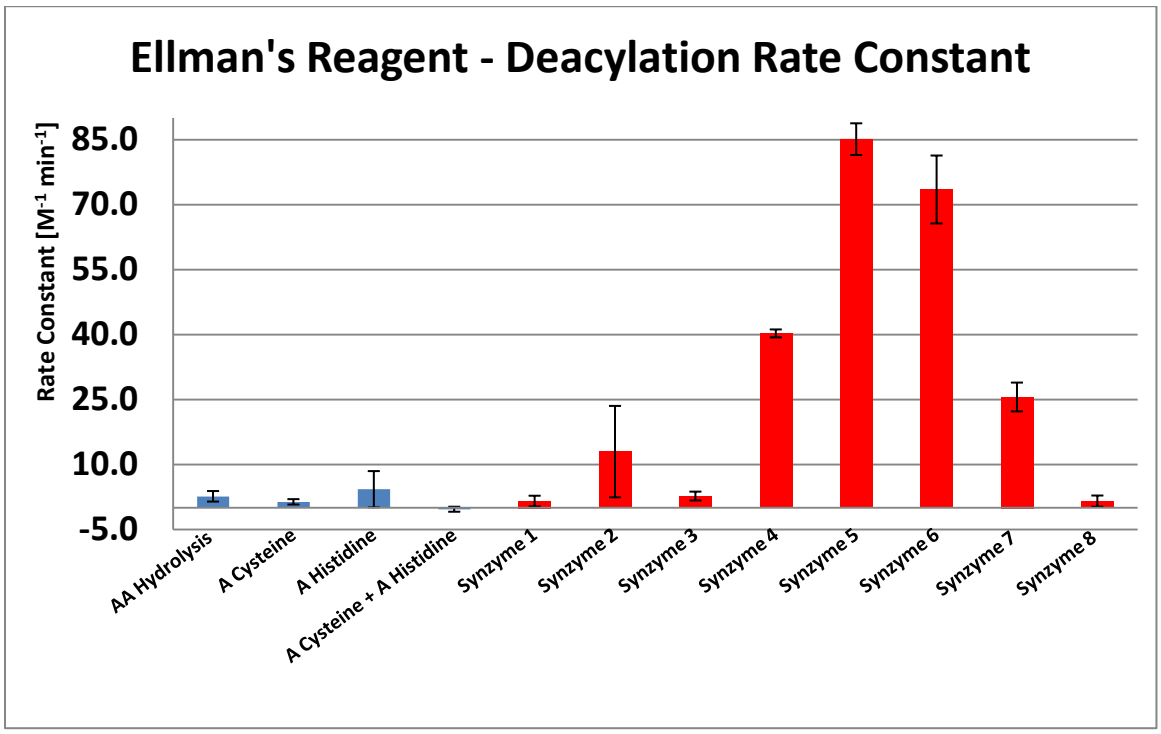

Figure 30 - Deacetylation rate constant of various synzyme.

5-3. NMR

Figure 31 and Figure 32 are the NMR spectra of free flowing acetyl cysteine and acetyl histidine respectively. The NMR half-height linewidth corresponding to the protons on the β-carbon of cysteine and the ε-carbon of histidine residues at 2.82 ppm and 8.43 ppm were used to compare to those on synzymes. The measurements corresponding to the half-height linewidth of each synzyme are shown in

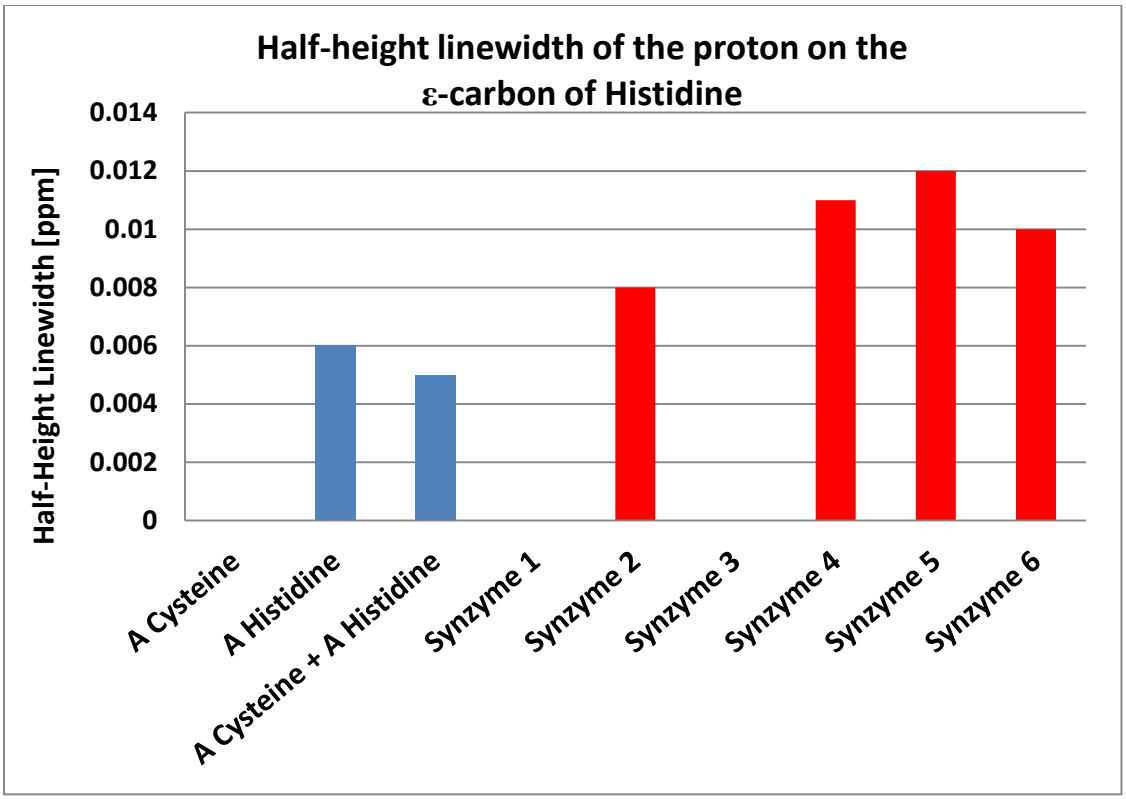

Figure 33 and Figure 34. Overall, the half-height linewidth of the synzyme appeared to have broadened, confirming there were indeed some interactions detected of the nuclei of interest with other side groups. In particular, synzymes with a phenylalanine between the cysteine and histidine residue, synzyme 5 and 6, the half-height linewidths were found to be slightly higher, confirming the steric hindrance effect created by the bulky side group brings the Cys-His closer together.

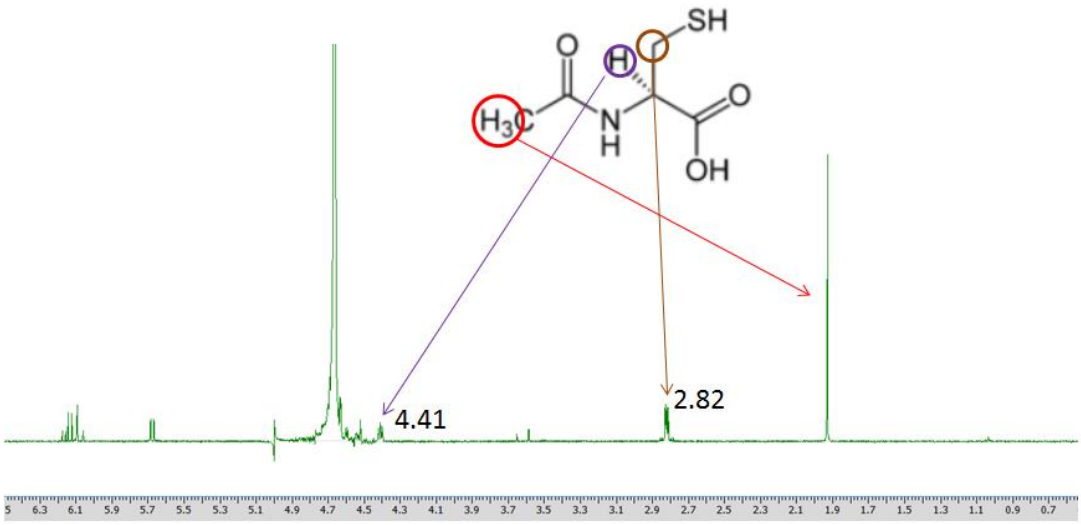

Figure 31 – 1D proton NMR spectra of acetyl cystidine.

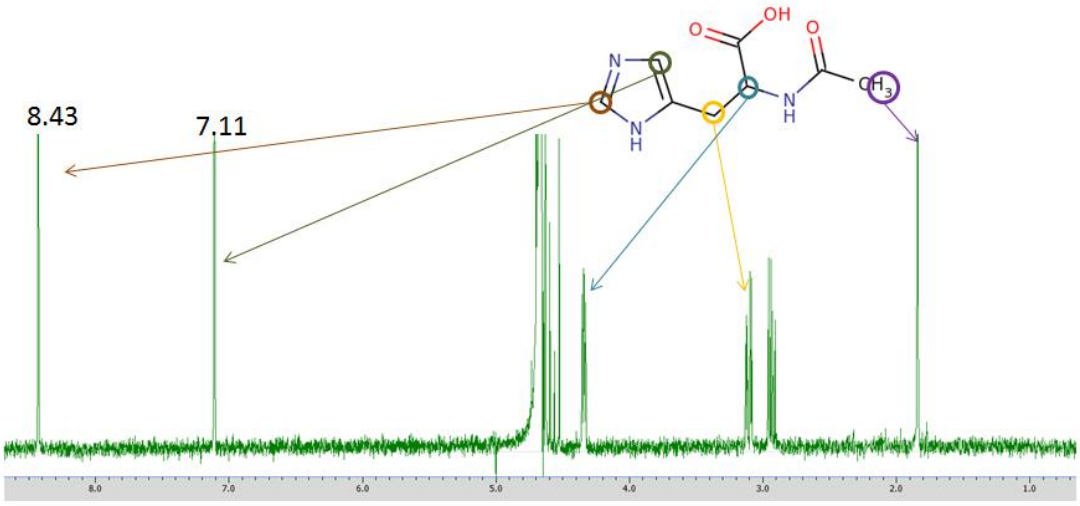

Figure 32 - 1D proton NMR spectra of acetyl histidine.

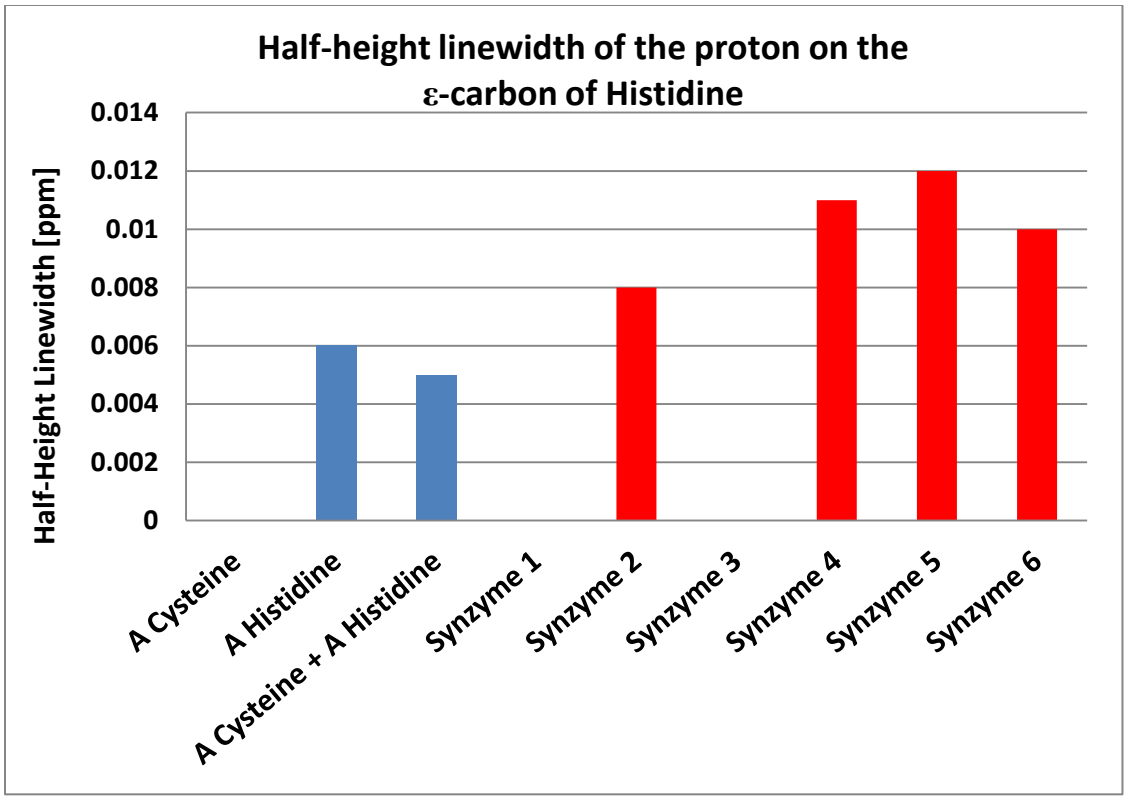

Figure 33 - Half-height linewidth of the proton on the ε-carbon of histidine.

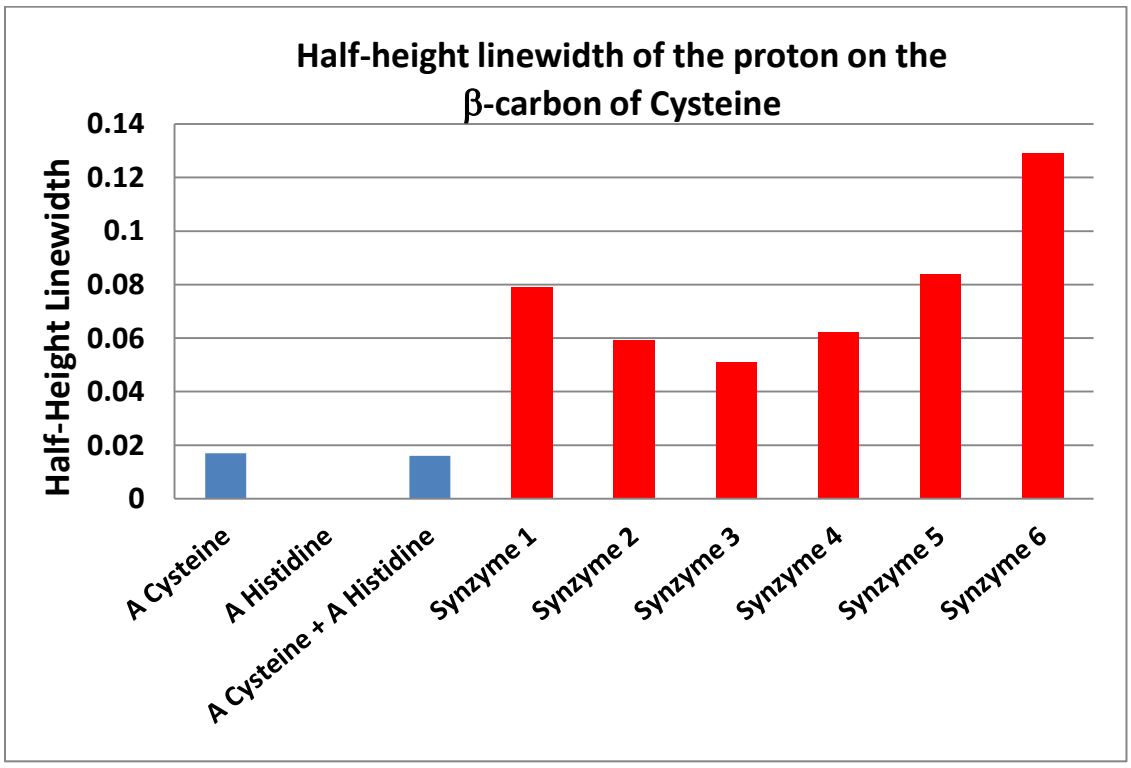

Figure 34 - Half-height linewidth of the proton on the b-carbon of cysteine.

5-4. Imidazole Added Buffer

Imidazole is a clear aid for deacylation as it helps remove the acetyl group from the thiol within the synzyme. To evaluate the effect of additional imidazole in aiding synzyme deacylation, we modified the buffer to have 1X, 10X, and 100X of imidazole relative to the synzyme concentration of 1E-4M. Figure 35 is the Ellman's Reagent absorbance measurement of synzyme 6 at 412nm for a 30-minute deacylation study. The plateau of the cleaved Ellman's Reagent absorbance at 10X and 100X imidazole concentration in buffer indicated all synzymes were deacetylated extremely rapidly. Hence, the time frame to measure the initial rate was shortened to the initial 30 seconds of the additional of the Ellman's Reagent as presented in Figure 36 - Numerical comparison of the deacylation rate of both synzyme 6 and acetyl cysteine/ acetyl histidine.For both control group and synzyme 6, deacylation rate is proportional to the ratio between imidazole and synzyme, confirming imidazole's overwhelming effect in aiding deacylation. Future synzyme design with addition histidine to aid deacylation requires further investigation.

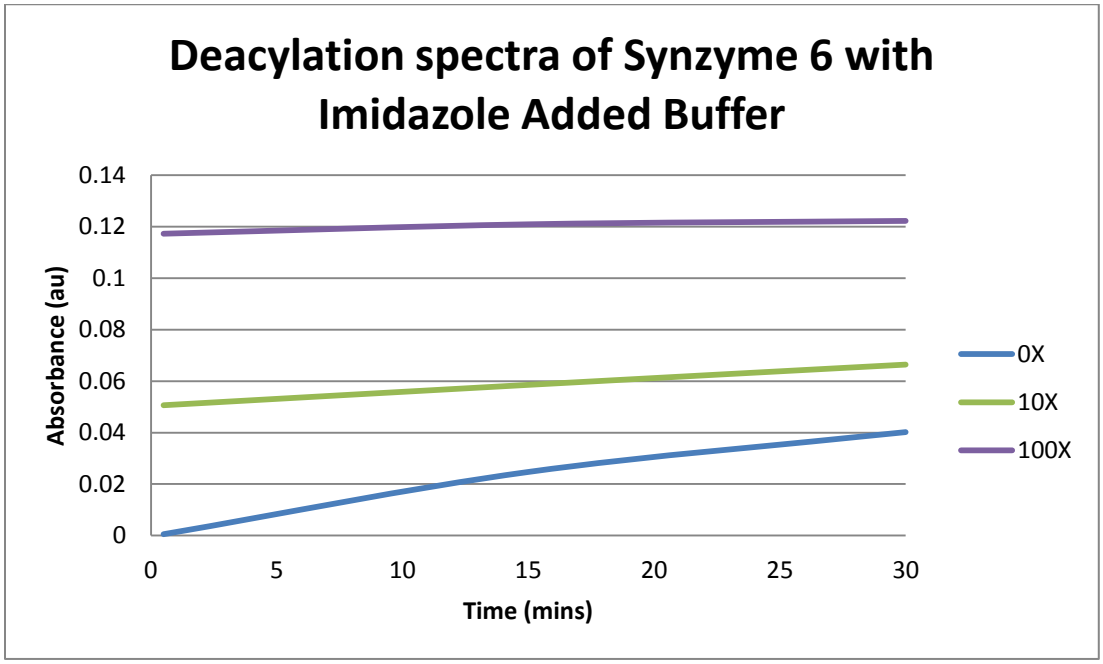

Figure 35 - Deacylation spectra of Synzyme 6 with Imidazole Added Buffer.

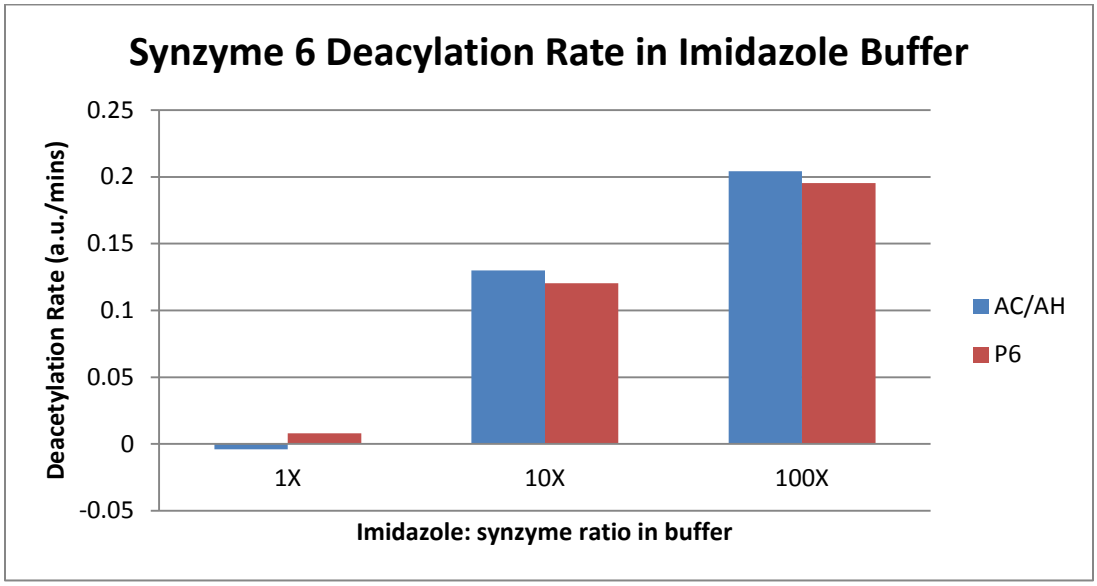

Figure 36 - Numerical comparison of the deacylation rate of both synzyme 6 and acetyl cysteine/ acetyl histidine.

5-5. Pulsing ** Proprietary Information for Thesis Review Only ***

To improve the catalysis of the synzyme, external electric field was used to induce dynamic motion during the acetyl-exchange. The reaction rates of the synzyme were tested with various electric field wave forms and compared to the rate without any electrical perturbation.

To examine the field strength to separate the charged triad residue during acetyl-exchange, synzyme 2 acetylation rate constant was studied at 1 kHz, sine wave setting at AC voltage amplitude ranging from 10V to 200V as shown in Figure 37. It was interesting to observe the decrease of acetylation rate with the increase of pulse strength starting at 20Vpp and significantly increases at 200Vpp. The significant jump in acetylation rate at 200Vpp was caused by the electrode heating at such voltage as observed with the melting of the electrode gel. The decrease

after 20Vpp suggests the possibility of locking the synzyme at certain structure state.

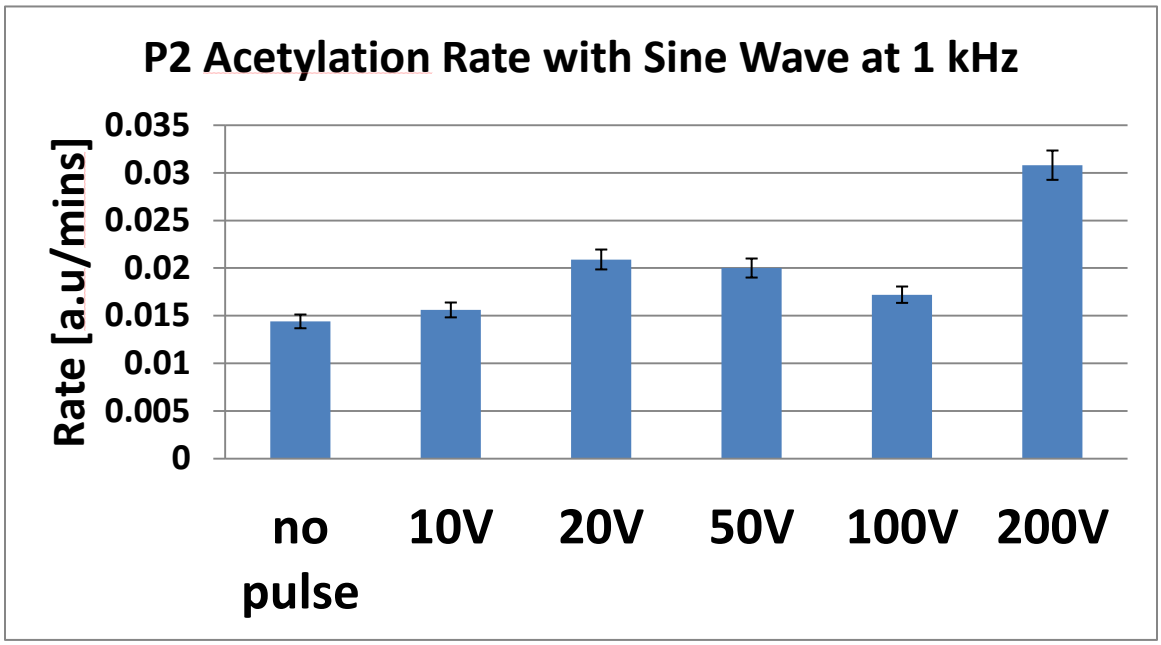

Figure 37 - Acetylation rate constant of synzyme 2 at different pulsing amplitude. * Proprietary Information for Thesis Review Only ***

Sine wave, square wave, arbitrary wave, and pulse wave at various frequency and amplitude were tested. Out of all the wave form tested, pulse electric field with 1% duty cycle and 10Vpp showed the most promising results in enhancing the acetylation rate. Figure 38 presented the acetylation rate constant of synzyme 6, 7 and the acetyl-cysteine/acetyl-histidine control at different pulsing frequency. The increase in synzyme 6 acetylation rate halted at 100 kHz, and rate began to decrease at higher frequency. T-test analysis of the synzyme 6 acetylation rate indicated a statistical significance for the 10 kHz and 100 kHz pulse electric field at a P value of 0.01. On the other hand, synzyme 7 and acetyl-cysteine/acetyl-histidine control did not exhibit the same dynamic property under pulsed electric field. This suggested that pulsing waveform, frequency, and possibly input pulse amplitude is specific to synzyme design. Furthermore, as

synzymes were free floating in homogenous solution, it was unclear on the portion of synzyme that was actually influenced by the electric field. Investigation in adding a constant offset voltage during non-pulsing time to align synzymes or bounding the synzyme onto solid surface is left for further studies.

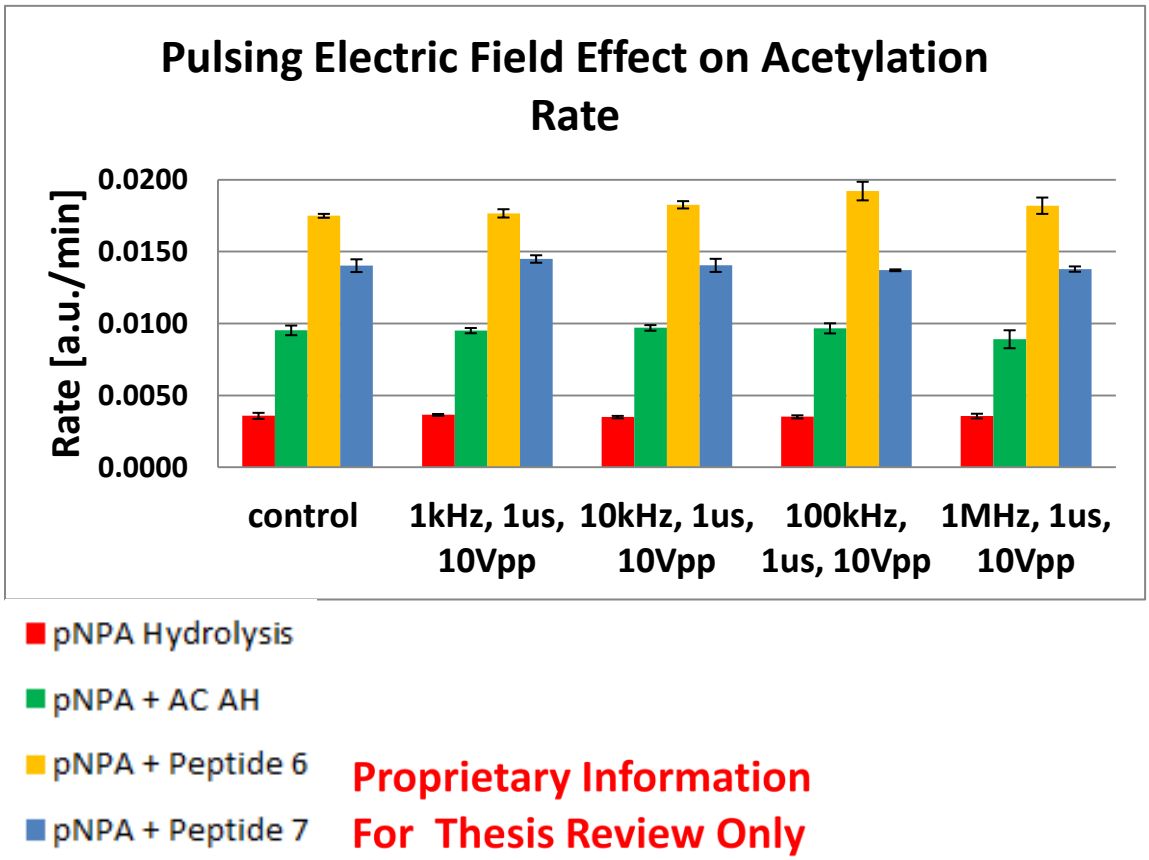

Figure 38 - Acetylation rate of synzyme 6, 7 and control under pulse electric field in input amplitude of 10Vpp and no offset voltage. * Proprietary Information For Thesis Review Only ***

5-6. Limitations

1. The oxidation of the synzymes overtime decreases the acetylation activity. Precaution measurement such as storing lyophilized synzyme at -20°C and calibrating its activity before experiments were taken to minimize the oxidation effect.

2. The size and the purity of the synzymes might contribute to the reduction in sensitivity of the NMR spectroscopy as nanoparticles contribute to a much lower magnetic moment for detection. (Noginova et al.)
3. As NMR measured average distance of the molecules, this effect in line-broadening due to closer interaction might have been damped. Also, NMR measures average time distance of molecules, which might have lessen the broadening effect of half-height linewidth created by the bending of synzyme.
4. Peaks in the NMR spectra could have been overlapped, leading to an overestimation of half-height linewidth. Magnitude of effects of substituents upon spectra shift fall off dramatically beyond alpha position, which could lead to misinterpretation of spectra as identical.
5. Non-uniformity of electrode fabrication due to electrode gel thickness leads to ~25% difference in overall electrode resistance and varies the applied electric field. This problem was overcome by reusing the same gel electrode within the same study. Studies show no significant change in performances with reusing gel within a single study which includes roughly 20 acetylation tests.
6. The maximum frequency output is limited by the output of the function generator.

CHAPTER 6: CONCLUSIONS

Proteases are involve in almost all human biochemical pathways as they efficiently and selectively breaks down peptide bonds, controlling protein size and degradation. Proteases are extremely complex 3D structures that execute precise control of reaction pathways with a rapid set of precise chemo-mechanical dynamic movements. While it is extremely difficult to mimic enzyme catalysis by replicating its 3D structure, it is possible to design nano-structures that contain some level of catalytic ability. To do so, the design of the nano-structure must be able to overcome the back-attack of the synzyme-substrate intermediate that prevents the thiol group from functioning effectively as a nucleophilic catalyst for hydrolysis.

In this research, synthetic enzymes were designed and synthesized using a combination of cysteine, histidine, serine, and aspartic acid to mimic the catalytic triad of cysteine protease. The synzyme acetylation and deacylation ability was examined with a series of enzyme-substrate reaction and Ellman's Reagent trapping study. Intramolecular interactions between synzyme functional groups study was made possible using 1D NMR Spectroscopy. An external pulse electric field was then applied to accelerate the efficiency of the catalytic process by inducing dynamic properties in the synzymes.

While none of the synzymes acetylated with p-Nitrophenol Acetate at a rate significantly greater than the controls, obvious difference was observed in deacylation rates for synzymes with one phenylalanine in between the triad, suggesting the large bulky R-group such as phenylalanine bends the backbone of the synzyme bringing the cysteine thiol group and the histidine imidazole group closer for acetyl exchange. Such enhancement effect was not observed with two phenylalanine placed in between the triad. This might due to the overcrowding of the triad, thus interfering with effective proton transfer during the acetyl-intermediate formation. NMR also confirmed the proximity effect of synzyme with additional phenylalanine.

Study in oscillating electric field suggested dynamic catalytic properties can be induced. The resonance frequency, input voltage amplitude, and wave form might be synzyme design dependent. Preliminary study in perturbing synzymes with oscillating electric field suggested pulse wave form at a frequency range of 10kHz to 100kHz and 20Vpp input voltage amplitude appeared to match the synzyme acetyl-exchange rate during deacylation and back attack. For synzyme 6, 15% increase in deacylation rate constant was observed. While this result is preliminary, it is still very encouraging to see statistical significant increase in catalysis rate simple linear synthetic enzyme design using electric perturbation.

6-1. Future Direction

Although the synzymes showed some level of catalytic ability with induced electric field, it design must be further optimized.

Synzyme design: Leveraging off the findings from the imidazole modified buffer deacylation test, new peptide design will incorporate multiple histidines to induce a “hand-off” effect. We envision the addition of the imidazole group will compete with the acetyl-thiol intermediate for a more efficient deacylation process. New synzyme designs with different charge distributions, dipole properties, and acid dissociation constants (pKa) will also be explored.

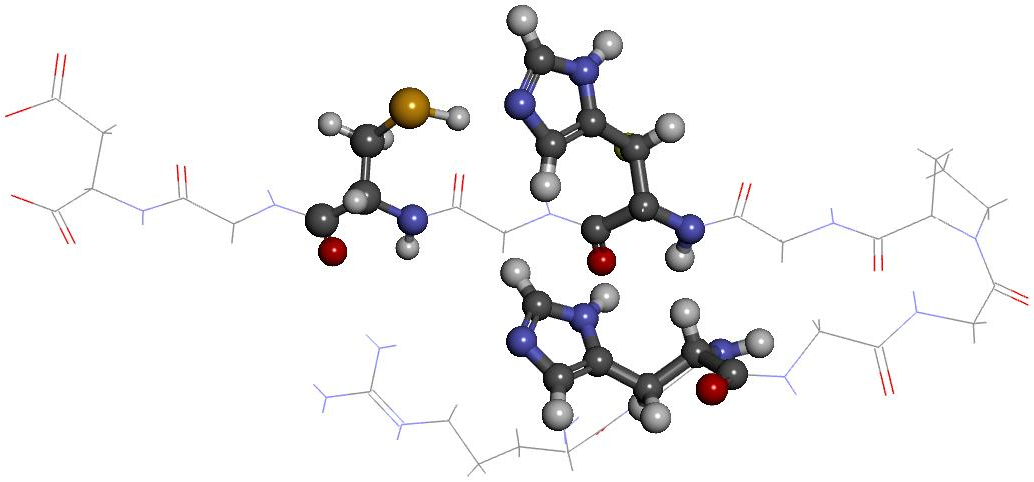

Figure 39 - Potential synzyme design with addition histidine.

Electrode design: The operating range of the function generator limited the output of the electrode. Thus, the impedance of the electrode was investigated as it played a critical role in the electric field profile.

Electric field input profile: Further investigation of the synzyme activity as a function of pulse electric field is necessary. In particular, a DC offset between pulsing will be implemented to align the synzymes, which in theory should enhance the pulsing effect. Multidimensional electric fields should yield higher spatial control of our molecules for manipulation, while anchoring the synzymes to a solid substrate can help reduce the degree of movement.

REFERENCES

Bachovchin, William W. “Review: Contributions of NMR spectroscopy to the study of hydrogen bonds in serine protease active sites.” *Magnetic Resonance in Chemistry* 39.S1 (2001): S199-S213. Web. 23 May 2012.

Banacky, P, Linder, B. “Model of Serine Proteases Charge Relay System - PCILO Study.” 13 (1981): n. pag. Print.

Beveridge, Allan J. “A theoretical study of the active sites of papain and S195C rat trypsin: Implications for the low reactivity of mytant serine proteinases.” (1996): 1355-1365. Print.

Chemistry, The Royal Society of. “Ultraviolet/visible spectroscopy.” *Modern Chemical Techniques*. 92. Print.

Deu, Edgar, Martijn Verdoes, and Matthew Bogyo. “New approaches for dissecting protease functions to improve probe development and drug discovery.” *Nature structural & molecular biology* 19.1 (2012): 9-16. Web. 5 Mar. 2012.

Ekici, A N, Mark Paetzel, and Ross E Dalbey. “Unconventional serine proteases : Variations on the catalytic Ser / His / Asp triad configuration.” (2008): 2023-2037.

Fricker, Simon P. “Cysteine proteases as targets for metal-based drugs.” *Metallomics : integrated biometal science* 2.6 (2010): 366-77. Web. 23 May 2012.

Heller, M J, J a Walder, and I M Klotz. “Intramolecular catalysis of acylation and deacylation in peptides containing cysteine and histidine.” *Journal of the American Chemical Society* 99.8 (1977): 2780-5.

Heller, Michael (Nanogen), Tu, Eugene (Nanogen), Sosnowski, Ronald (Nanogen), O’Connell, James (Nanogen). “Methods for electronic fluorescent perturbation for analysis and electronic perturbation for catalysis for synthesis.” 2000 : n. pag. Print.

Holman, Theodore (UC Santa Cruz). “Nuclear Magnetic Resonance Spectroscopy of Paramagnetic Substances in Solution.” *CHEM 256B Lecture*. Print.

Hunter, T. “Protein kinases and phosphatases: the yin and yang of protein phosphorylation and signaling.” *Cell* 80.2 (1995): 225-36.

Janowski, Robert (Adam Mickiewicz University). “Catalytic Triad.” Web. 6 Jan. 2012.

Kisailus, David et al. “Self-assembled bifunctional surface mimics an enzymatic and templating protein for the synthesis of a metal oxide semiconductor.” *Proceedings of the National Academy of Sciences of the United States of America* 103.15 (2006): 5652-7.

Kopeliovich, Dmitri. “Diffusion layer.” Web. 6 Jan. 2012.

Kraut, J. “Serine proteases: structure and mechanism of catalysis.” *Annual review of biochemistry* 46 (1977): 331-58.

Liao, Debbie et al. “Synthetic enzyme inhibitor: a novel targeting ligand for nanotherapeutic drug delivery inhibiting tumor growth without systemic toxicity.” *Nanomedicine : nanotechnology, biology, and medicine* 7.6 (2011): 665-73. Web. 22 May 2012.

NMRCentral. “Chemical Shift.” 2011. Web. 6 Jan. 2012.

Nelson, David, Cox, Michael. *Lehninger Principles of Biochemistry*. 5th ed. W. H. Freeman, 2008. Print.

Noginova, N et al. “NMR and spin relaxation in systems with magnetic nanoparticles: effects of size and molecular motion.” *Journal of physics. Condensed matter : an Institute of Physics journal* 21.25 (2009): 255301. Web. 12 Apr. 2012.

“Nuclear Magnetic Resonance Spectroscopy.” Web. 6 Jan. 2012.

Polgár, L, and P Halász. “Current problems in mechanistic studies of serine and cysteine proteinases.” *The Biochemical journal* 207.1 (1982): 1-10.

Rawlings, Neil D, Fraser R Morton, and Alan J Barrett. “MEROPS: the peptidase database.” *Nucleic acids research* 34.Database issue (2006): D270-2. Web. 18 Mar. 2012.

Shen, Hong-Bin, and Kuo-Chen Chou. “Identification of proteases and their types.” *Analytical biochemistry* 385.1 (2009): 153-60. Web. 13 Apr. 2012.

Techniques, Modern Chemical. “2 . Nuclear magnetic resonance spectroscopy.” 30-61. Print.

Tsong, T Y, and R D Astumian. “Electroconformational coupling and membrane protein function.” *Progress in biophysics and molecular biology* 50.1 (1987): 1-45.

Tsong, Yow Tsong, Liu, Dao-Sheng, Chauvin, Francoise. “Electroconformational coupling: an electric field induced enzyme oscillation for cellular energy and signal transductions.” 21.October 1988 (1989): 319-331. Print.